

Supplementary Information

Three New Stigmatellin Derivatives Reveal Biosynthetic Insights of its Side Chain Decoration

Dorothy A. Okoth ^{1,2+}, Joachim J. Hug ^{1,2,3+}, Ronald Garcia ^{1,2,3} and Rolf Müller ^{1,2,3*}

1 Helmholtz-Institute for Pharmaceutical Research Saarland (HIPS), Helmholtz Centre for Infection Research (HZI) and Department of Pharmacy, Saarland University, Campus E8 1, 66123 Saarbrücken, Germany

2 German Center for Infection Research (DZIF), Partner Site Hannover-Braunschweig, 38124 Braunschweig, Germany

3 Helmholtz International Labs, Department of Microbial Natural Products, Saarland University, Campus E8 1, 66123 Saarbrücken, Germany

* Correspondence: rolf.mueller@helmholtz-hips.de; Tel.: +49-681-98806-3000

+ These authors contributed equally to this work.

Table of Contents

1. LC-MS analysis	3
1.1 Partial ESI-MS spectra.....	3
1.2 MS ² spectra	6
1.3 Proposed fragmentation pattern of 1–4	12
1.4 Alternative producer investigation of 1–4	16
2. NMR spectroscopic data.....	17
3. Biosynthetic <i>in silico</i> investigation	21
4. ¹ H and ¹³ C NMR spectra.....	25
5. References	47

1. LC-MS analysis

1.1 Partial ESI-MS spectra

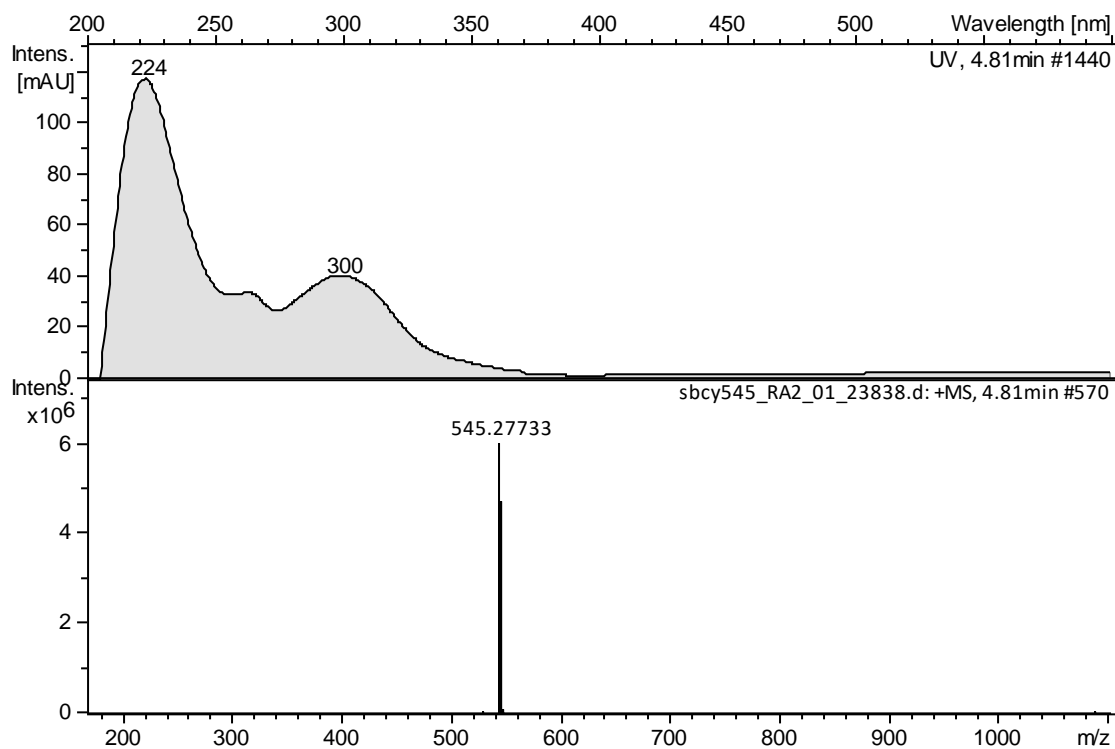


Figure S1. UV/VIS and partial ESI+MS spectra of purified stigmatellic acid (**1**).

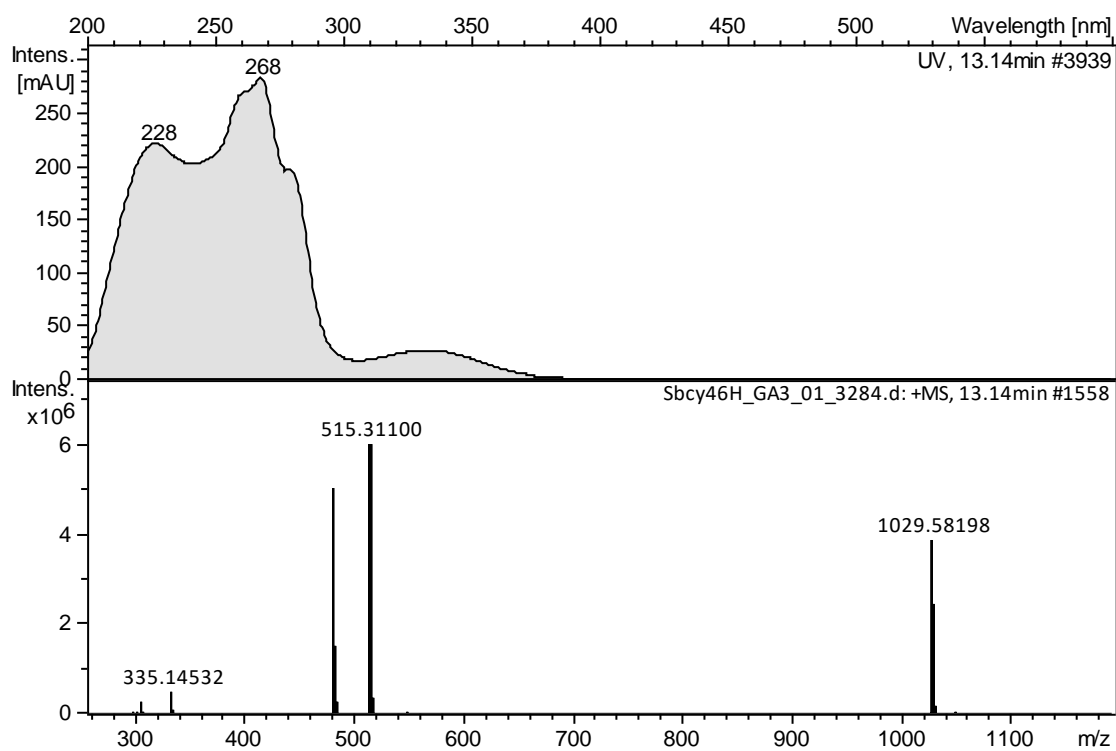


Figure S2. UV/VIS and partial ESI+MS spectra of purified *iso*-methoxy stigmatellin (**2**).

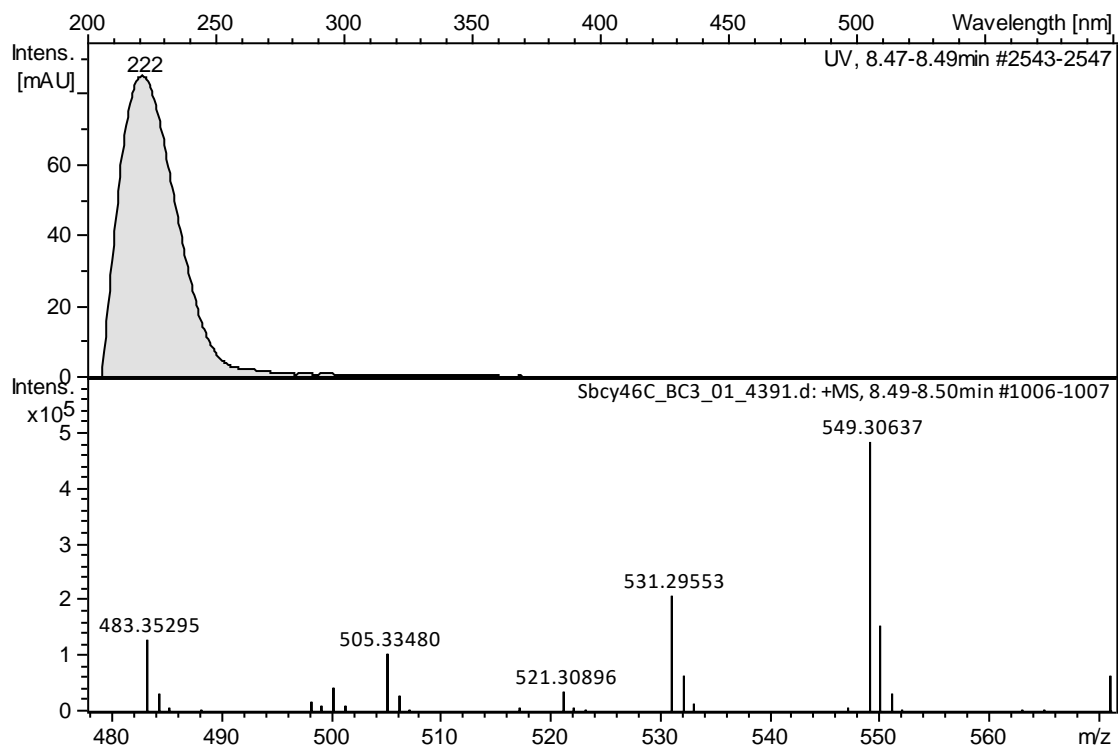


Figure S3. UV/VIS and partial ESI+MS spectra of purified stigmatellin C (isomer 1, **3**).

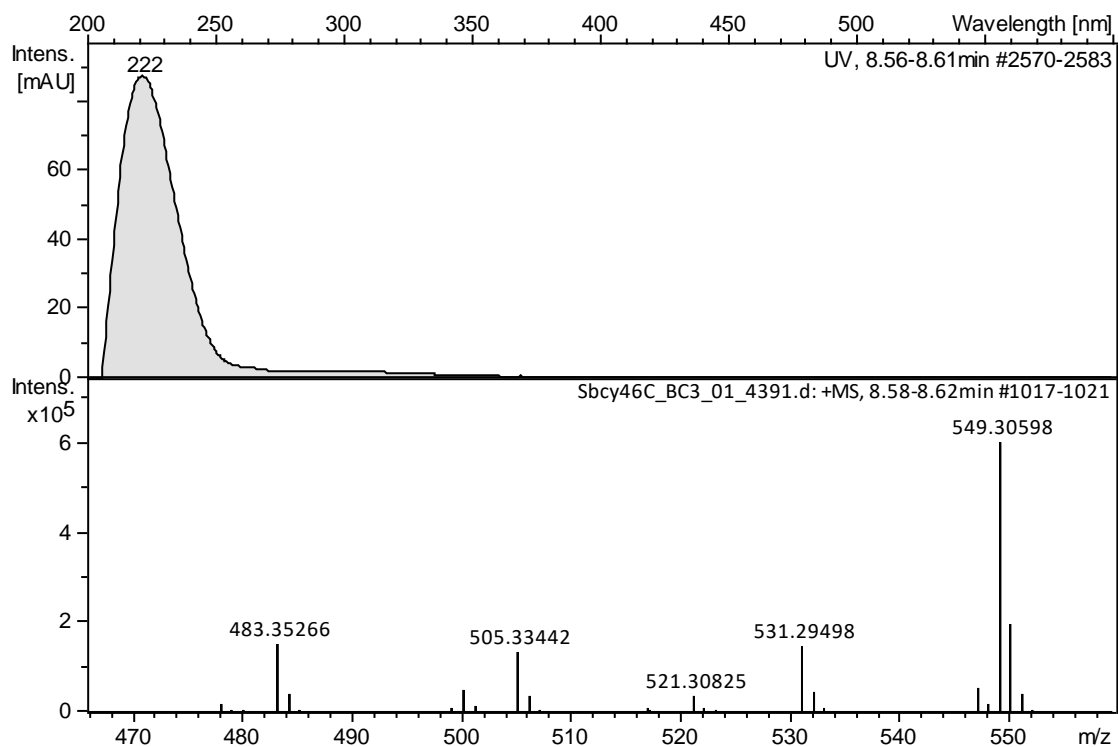


Figure S4. UV/VIS and partial ESI+MS spectra of purified stigmatellin C (isomer 2, **3**).

1.2 MS² spectra

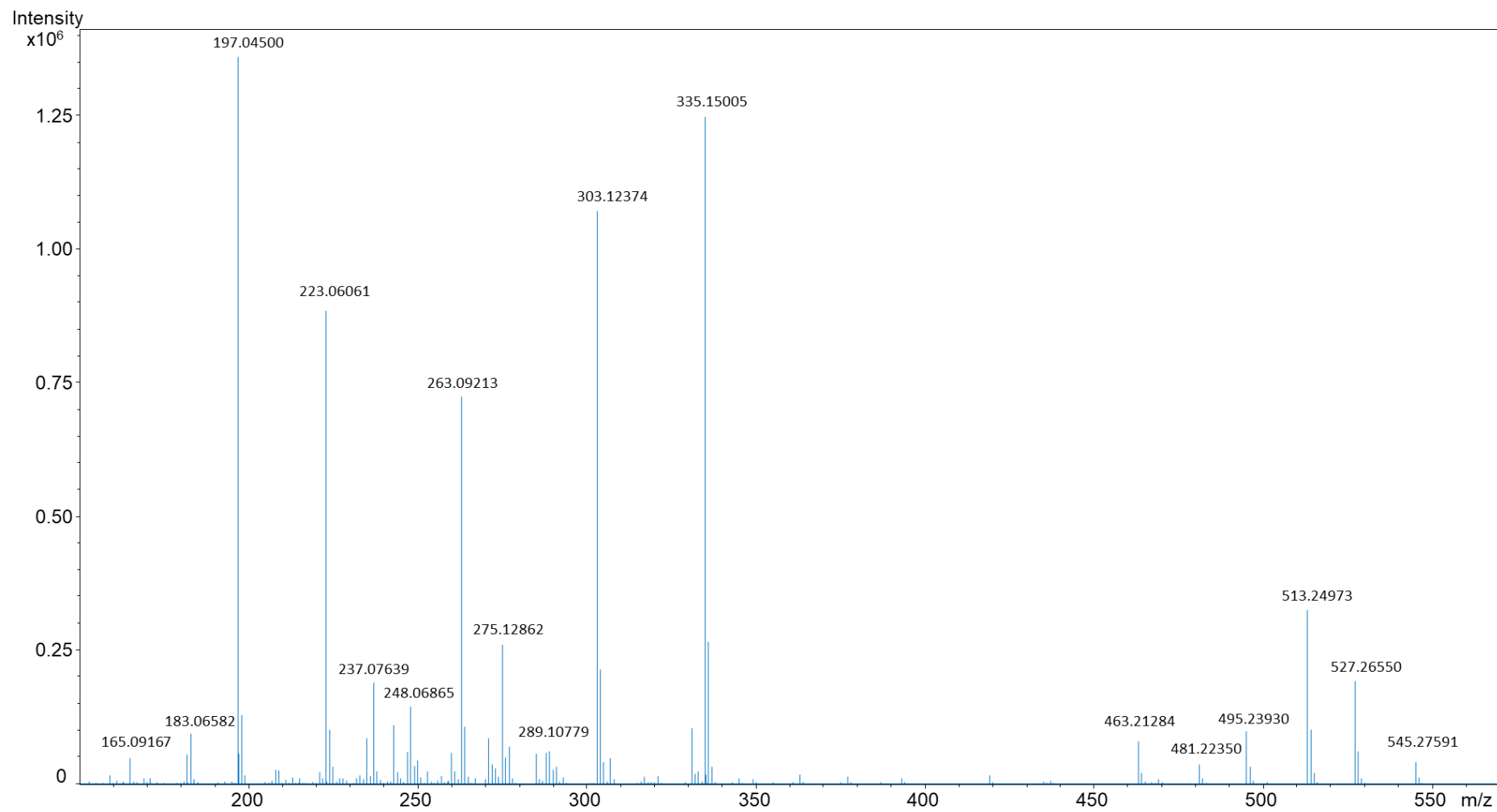


Figure S5. Fragmentation pattern in ESI+MS² experiment of stigmatellic acid (**1**).

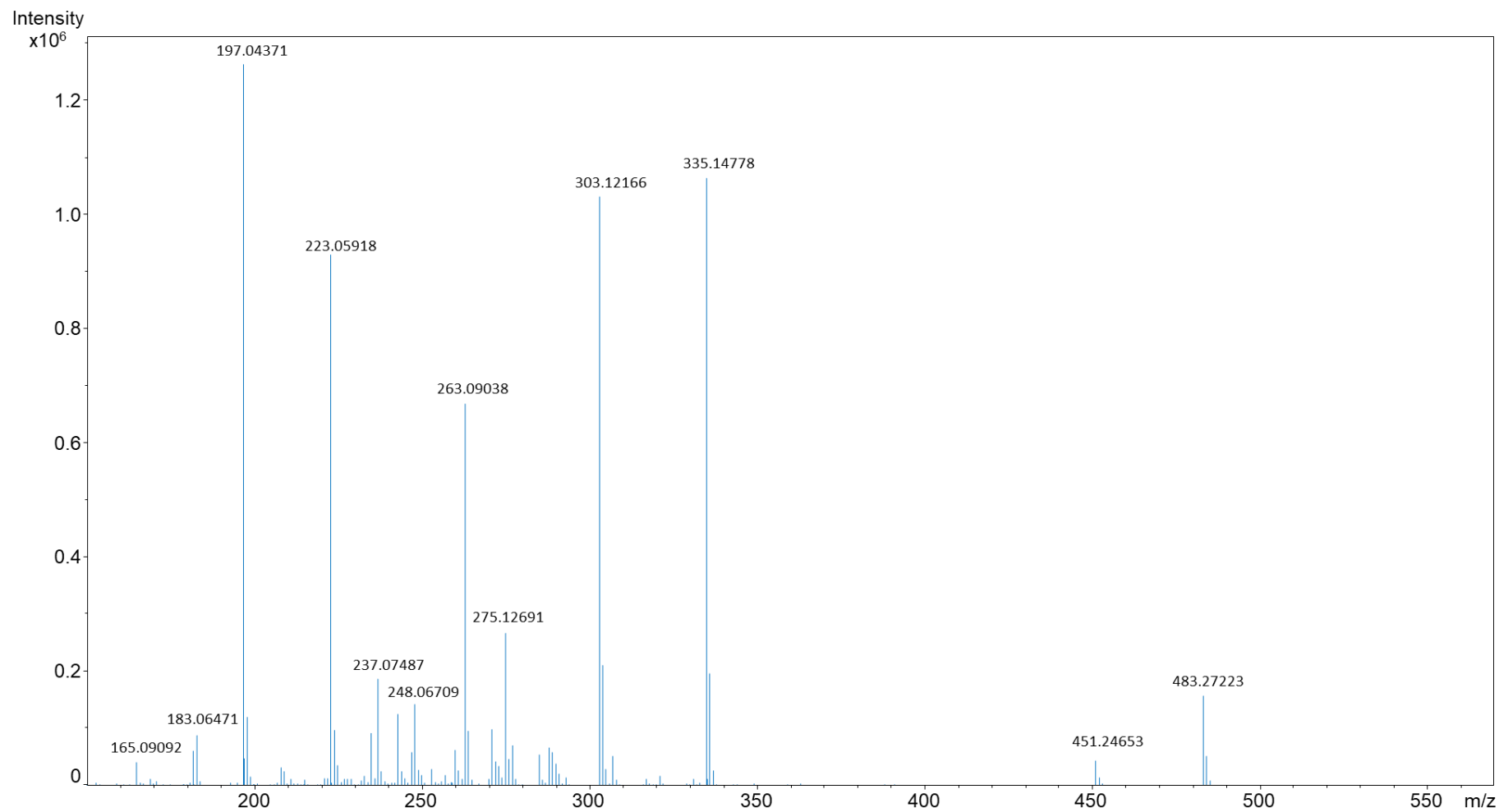


Figure S6. Fragmentation pattern in ESI+MS² experiment of *iso*-methoxy stigmatellin A (**2**).

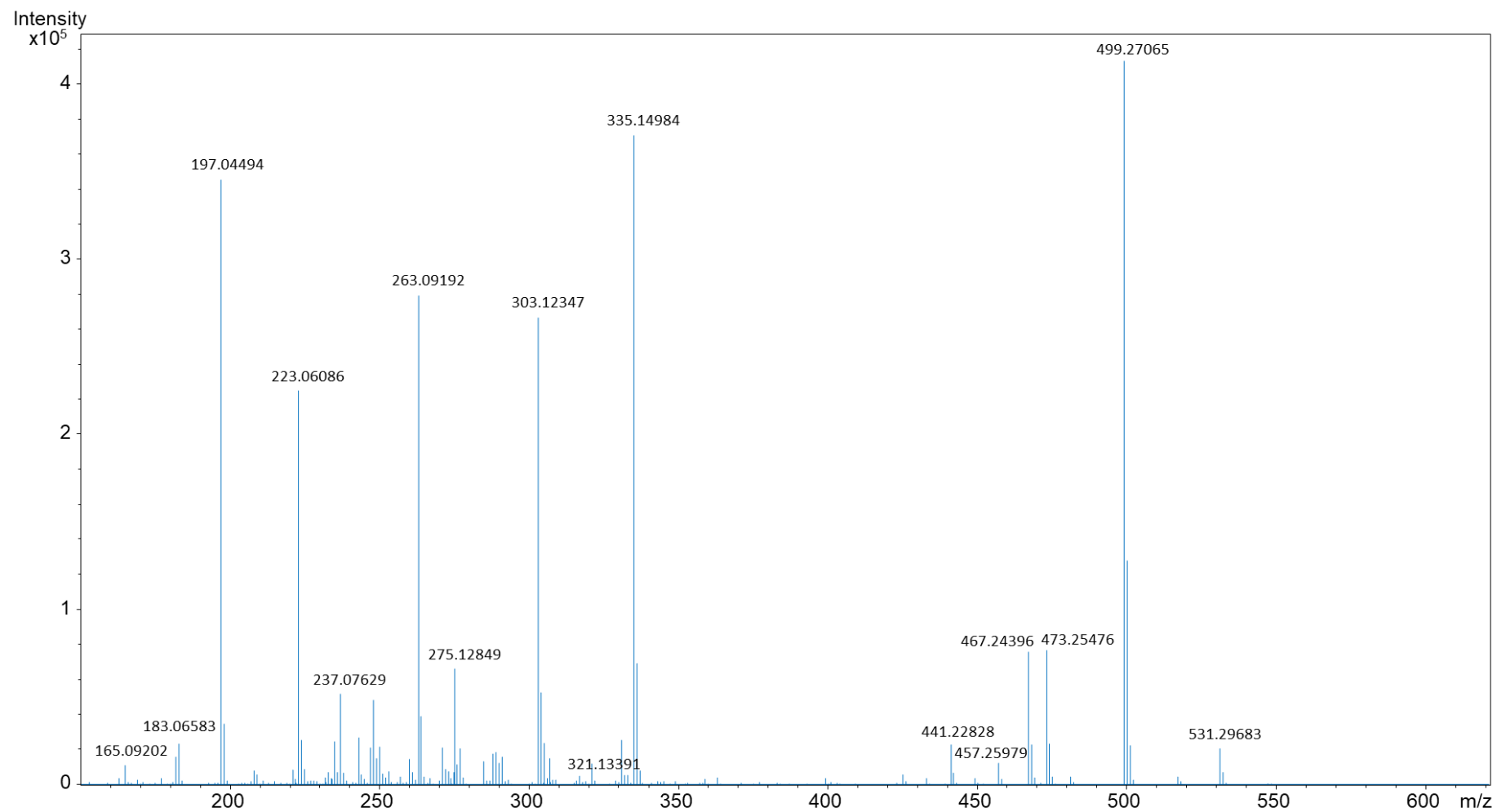


Figure S7. Fragmentation pattern in ESI+MS² experiment of stigmatellin C (isomer 1, 3).

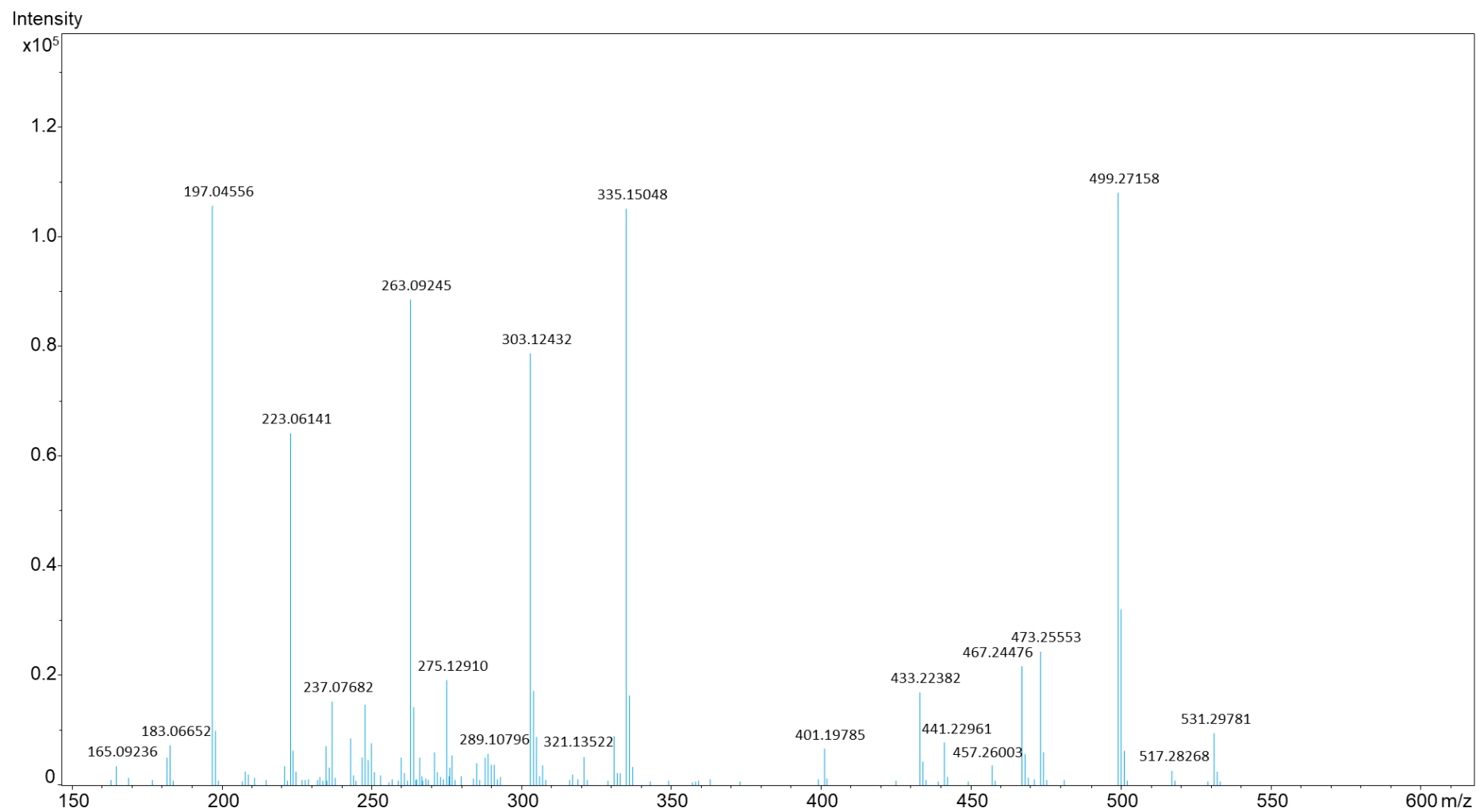


Figure S8. Fragmentation pattern in ESI+MS² experiment of stigmatellin C (isomer 2, 3).

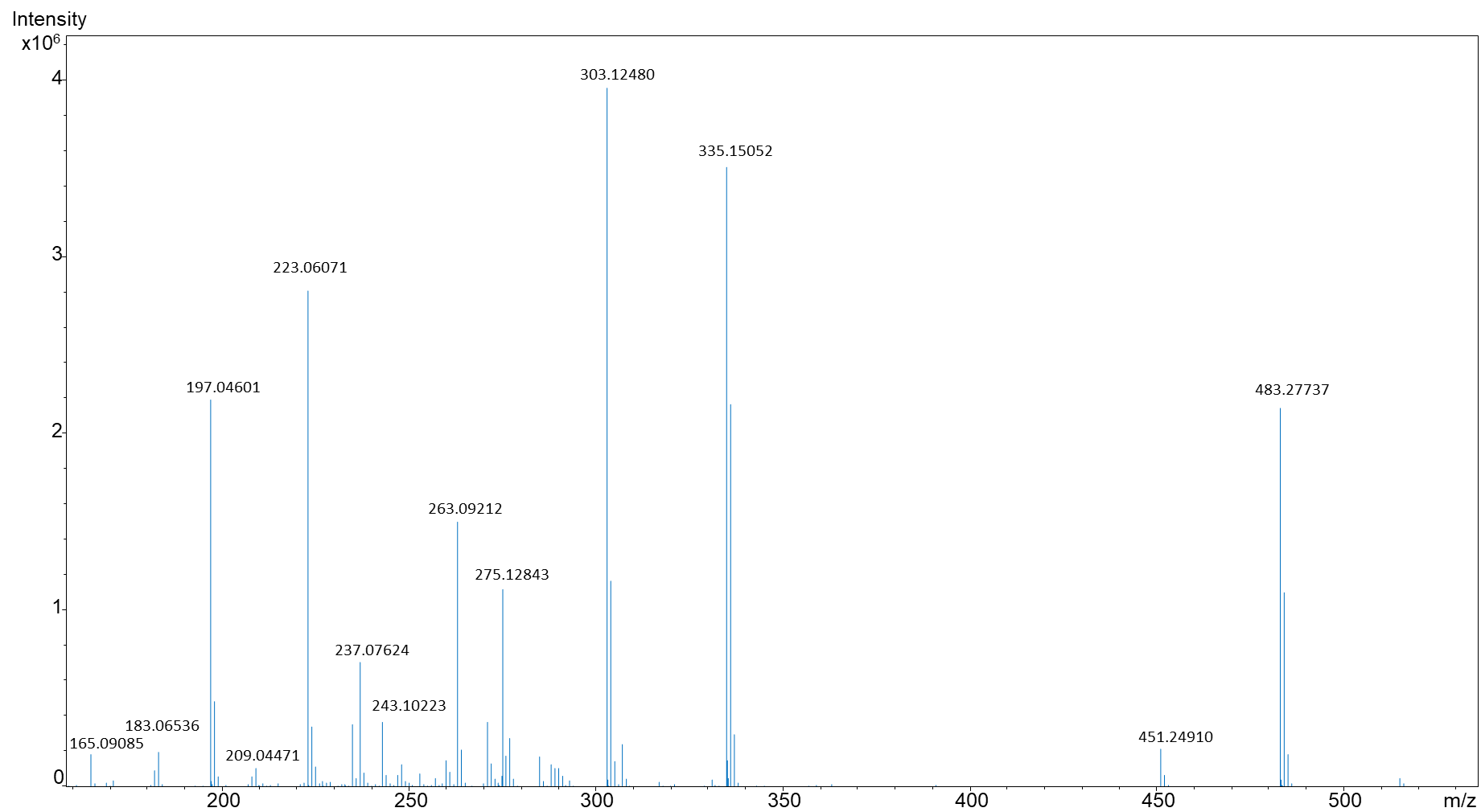


Figure S9. Fragmentation pattern in ESI+MS² experiment of stigmatellin A (**4**).

1.3 Proposed fragmentation pattern of 1–4

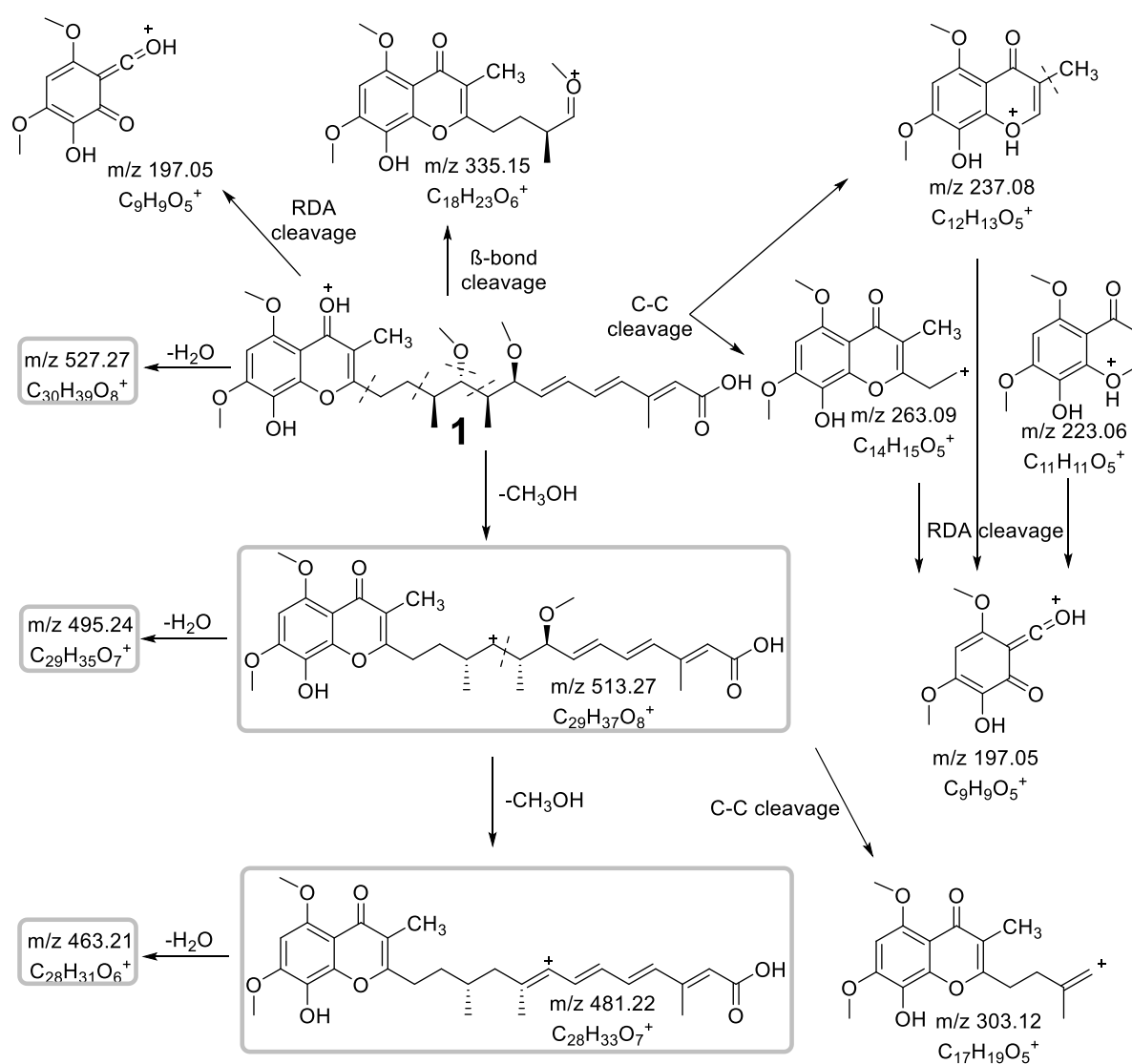


Figure S10. MS² fragmentation scheme of **1** and proposed structure of identified key ion fragments (ion fragments in grey box are specific for **1**). RDA: retro-Diels Alder.

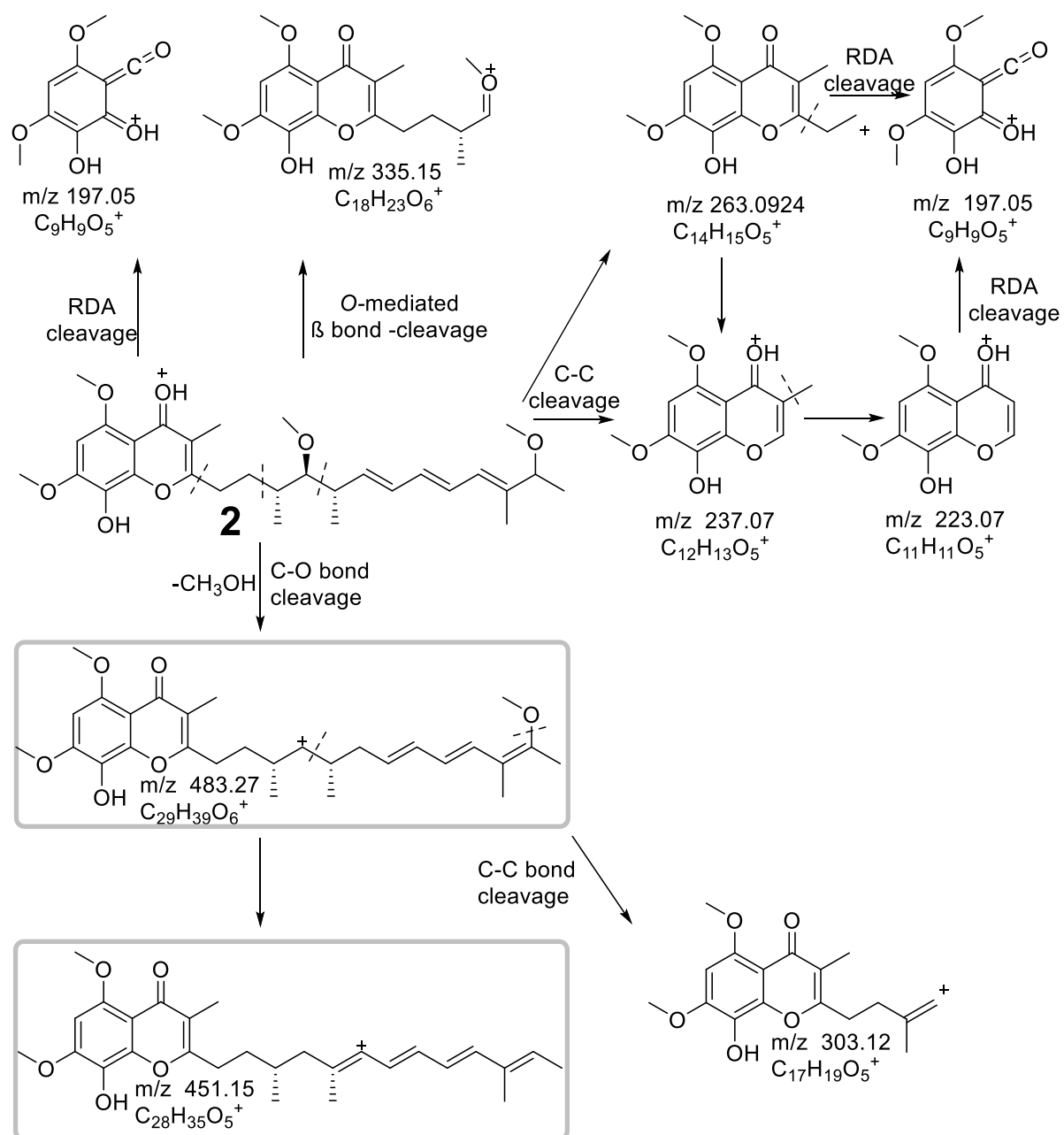


Figure S11. MS² fragmentation scheme of **2** and proposed structure of identified key ion fragments (ion fragments in grey box have been observed specifically for **2** and **4**). RDA: retro-Diels Alder.

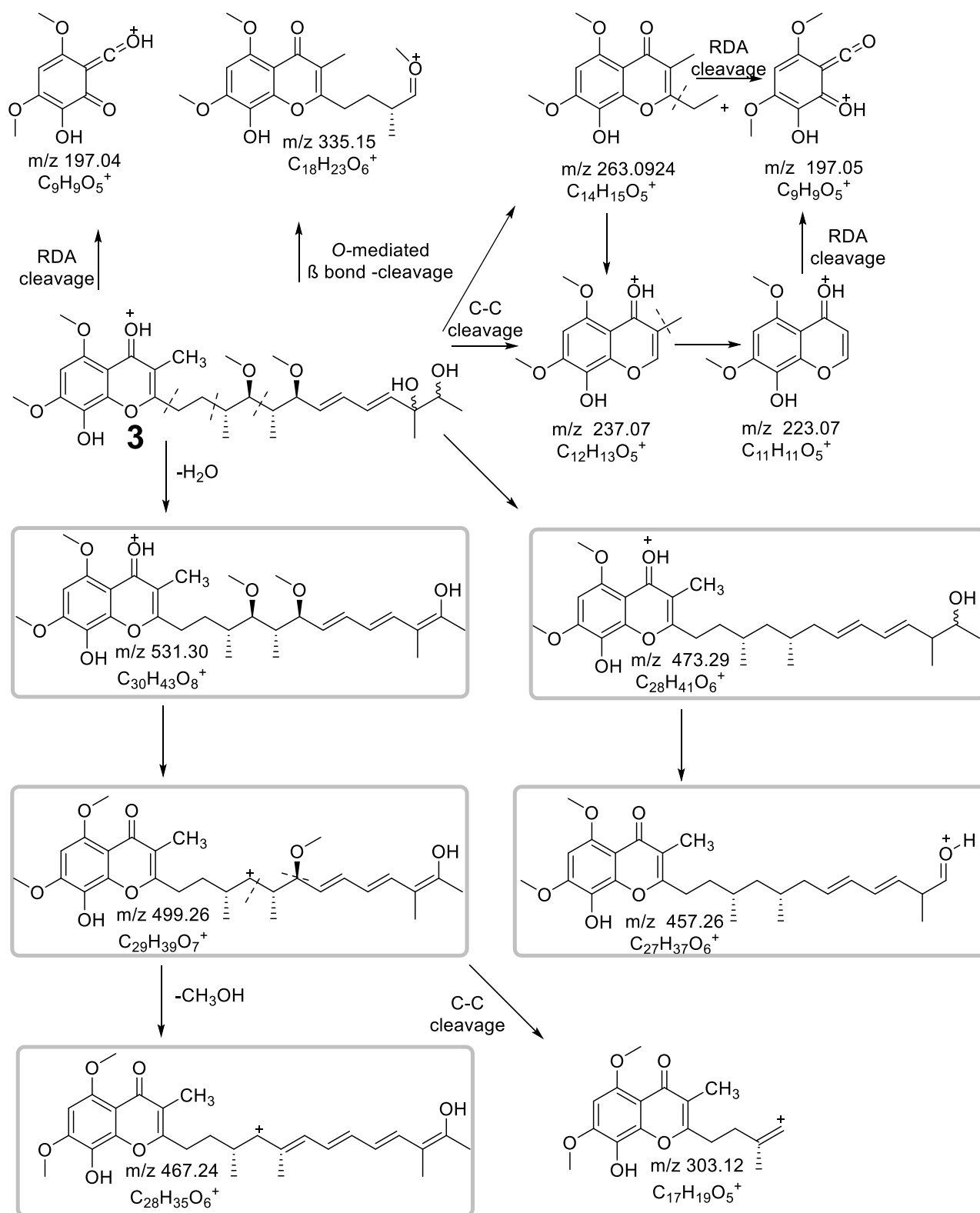


Figure S12. MS² fragmentation scheme of **3** and proposed structure of identified key ion fragments (ion fragments in grey box are specific for **3**). RDA: retro-Diels Alder.

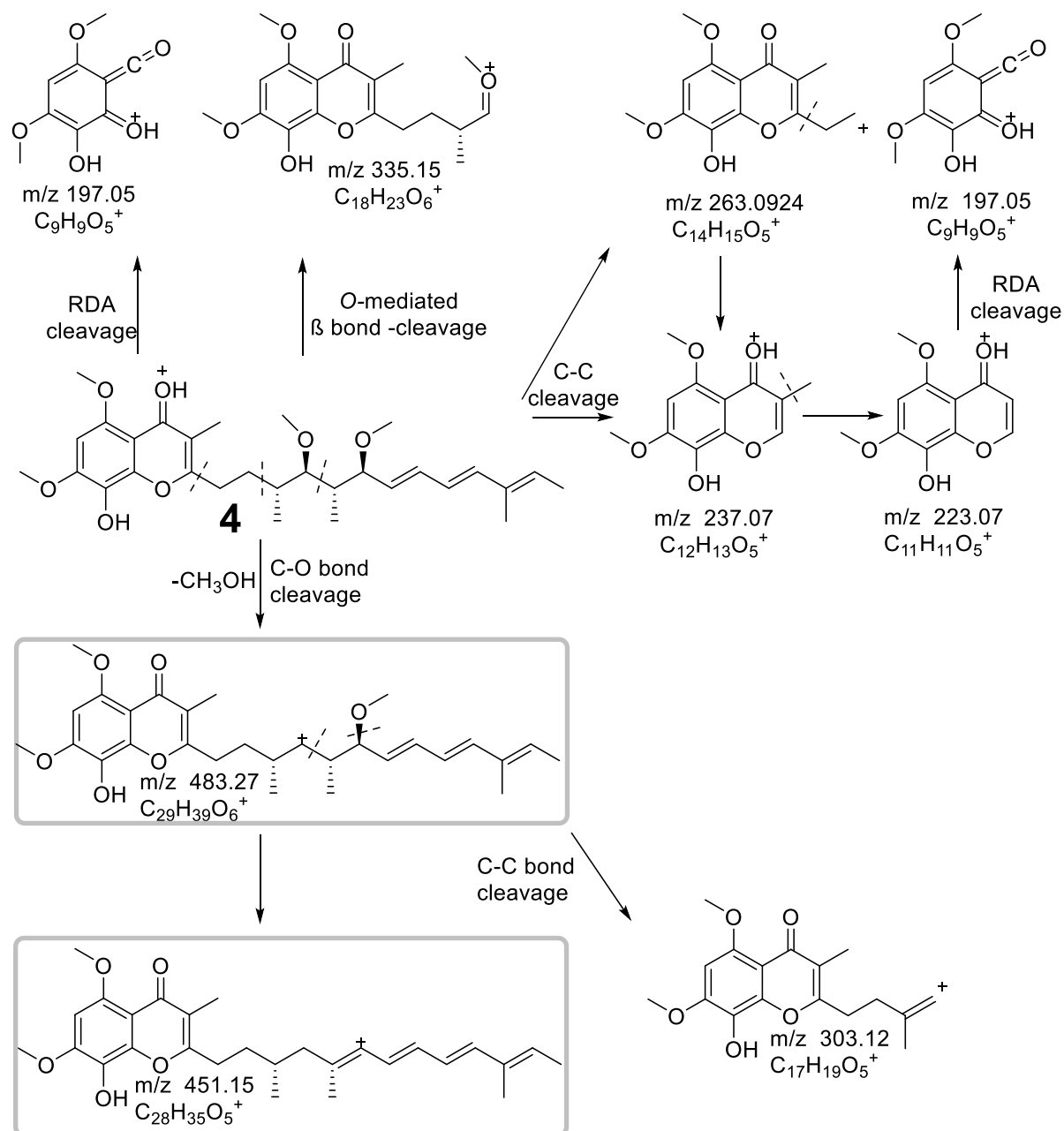


Figure S13. MS² fragmentation scheme of **4** and proposed structure of identified key ion fragments (ion fragments in grey box have been observed specifically for **2** and **4**). RDA: retro-Diels Alder.

1.4 Alternative producer investigation of 1–4

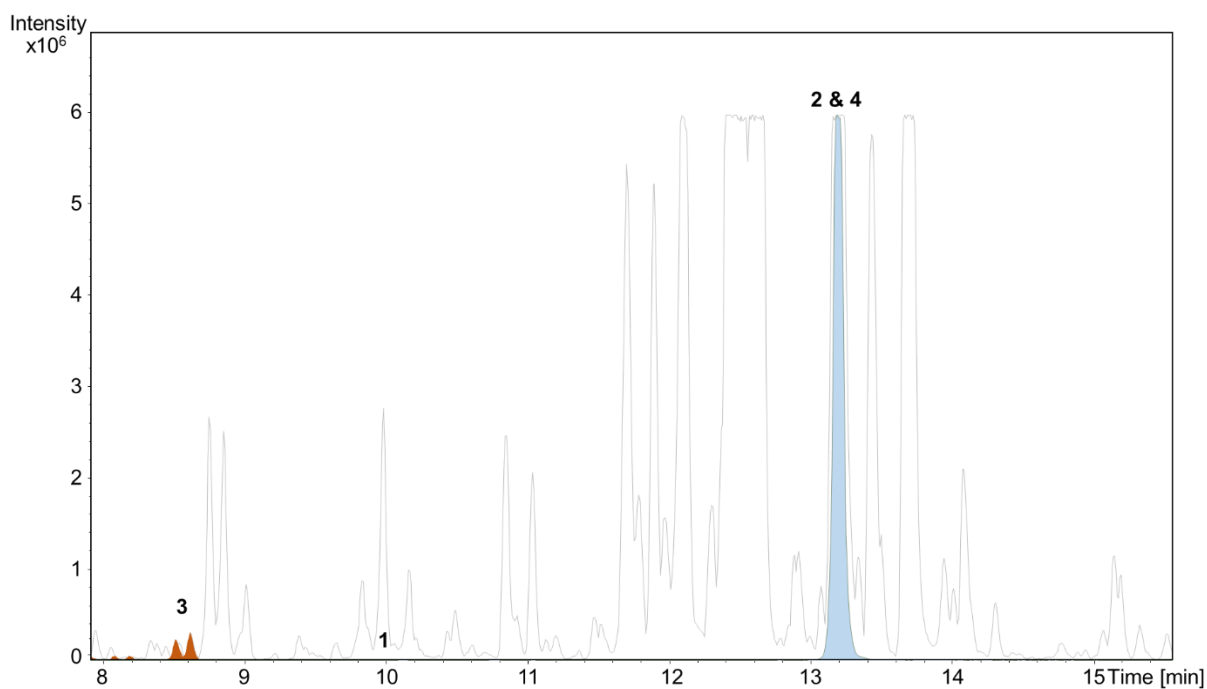


Figure S14. High performance liquid chromatography–mass spectrometry base peak chromatogram (HPLC–MS BPC) (grey) and extracted ion chromatograms (EICs) of **1** ($[M+H]^+$ 545.2755 m/z, green (not visible)), **2** ($[M+H]^+$ 515.3004 m/z, blue), **3** ($[M+H]^+$ 549.3064 and 549.3060 m/z, brown), and **4** ($[M+H]^+$ 545.2755 m/z, blue) from *Stigmatella aurantiaca* Sg a15.

2. NMR spectroscopic data

Table S1. Spectroscopic values of stigmatellic acid (**1**) acquired in methanol- d_4 at 700 MHz.

Stigmatellic acid (1)					
Position	δ_c	δ_H , [m, J (Hz)]	COSY	HMBC	ROESY
1a	148.2	-	-	-	-
2	165.6	-	-	-	-
3	117.5	-	-	-	-
4	179.9	-	-	-	-
4a	108.4	-	-	-	-
5	154.0	-	-	-	-
6	93.9	6.62 s 1H	-	1a, 4a, 4, 5,8, 7,	H-5-O-, H-7-O-
7	152.7	-	-	-	-
8	129.1	-	-	-	-
9	10.2	1.98 s 3H	-	2, 3, 4	-
1'	30.6	2.84 m 1H 2.69 m 1H	H-2'	2, 3, 2', 3'	-
2'	28.3	1.92 m 1H 1.55 m 1H	H-3'	2, 1', 3',4' 14'	-
3'	35.6	1.71 m 1H	H-14'	1',2',4', 15'	-
4'	88.7	3.11 dd 1H (2.3/9.4)	H-3'	2', 3', 5', 6',14', 15', 4'-OCH ₃ , 6'-OCH ₃	H-14', H-15'
5'	42.9	1.68 m 1H	H-15'	4', 15'	-
6'	82.4	3.94 dd 1H (2.5/7.0)	H-5', H-7'	4', 5', 7', 8', 15', 6'O-	H-3', H-5'
7'	138.3	5.86 dd 1H (7.0/15.6)	H-6', H-8'	5', 6', 9'	-
8'	133.3	6.31 dd 1H (10.5/15.3)	H-9'	6', 9', 10'	-
9'	135.2	6.71 dd 1H (10.5/15.3)	H-8',H-10'	7', 8', 11'	H-7', H-16'
10'	136.8	6.32 d 1H (15.3)	H-9'	8', 9', 11', 12', 16'	H-6', H-8', H-12'
11'	153.4	-	-	-	-
12'	121.1	5.81 s 1H	-	10', 11', 13', 16'	H-10'
13'	170.8	-	-	-	-
14'	18.4	1.15 d 3H (6.9)	H-3'	2', 3', 4'	-
15'	10.6	0.72 d 3H (7.1)	H-5'	4', 5', 6'	-
16'	14.0	2.28 d 3H (1.1)	-	10', 11', 12', 13'	-
5O-	56.8	3.88 s 3H	-	5,6	-
7O-	57.1	3.98 s 3H	-	7	-
4'O-	62.0	3.47 s 3H	-	4'	-
6'O-	57.0	3.24 s 3H	-	6'	-

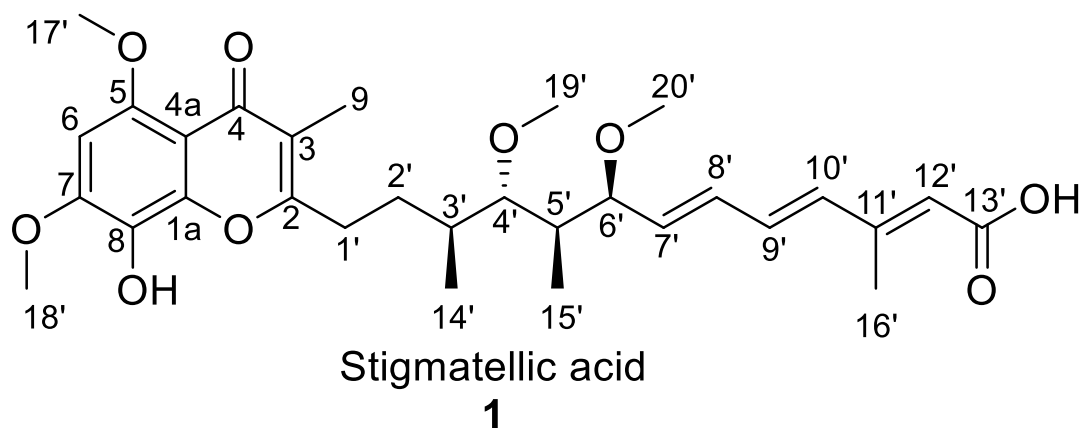
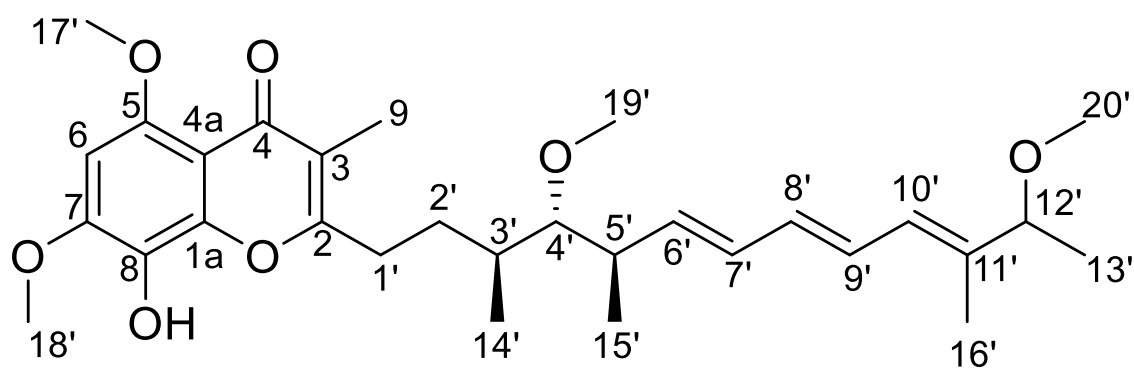


Table S2. Spectroscopic values for *iso*-methoxy stigmatellin (**2**) acquired in methanol- d_4 at 700 MHz.

<i>Iso</i> -methoxy-stigmatellin (2)				
Position	δ_c	δ_H , [m, <i>J</i> (Hz)]	COSY	HMBC
1a	148.1	-	-	-
2	165.5	-	-	-
3	117.2	-	-	-
4	179.7	-	-	-
4a	108.2	-	-	-
5	153.9	-	-	-
6	93.8	6.62 s 1H	-	4a,5,7 8, 1a,
7	152.5	-	-	-
8	128.9	-	-	-
9	9.9	1.98 s 3H	-	1', 2, 3,4
1'	30.6	2.84 m 1H 2.69 m 1H	H-2'	2',3', 2,3
2'	30.4	2.06 m 1H 1.56 m 1H	H-3'	1', 3', 4',14',
3'	37.2	1.67 m 1H (1.1)	H-14'	1',2', 4',14'
4'	91.6	2.86 m 1H	H-3',H-5'	2', 3', 5', 6', 4'-O-, 14',15'
5'	41.3	2.51 m 1H	H-6'	4', 6',7',15'
6'	137.7	5.69 m 1H	H-7'	4',5',7',8',15'
7'	132.1	6.14 dd 1H	H-6',H-8'	5', 6',8',9'
8'	127.7	6.36 m 1H	H-7',H-9'	6', 7',9',10'
9'	134.5	6.14,m, 1H	H-8',H-10'	7',8',10', 11'
10'	128.4	6.01, d, 1H(11.0)	H-9'	8',9',11'12',16'
11'	138.7	-	-	-
12'	83.9	3.37 s 1H (6.4)	H-13'	10',11'12'-O-,13',16',
13'	20.3	1.21 dd 3H (0.5/6.4)	H-12'	11';12'
14'	16.8	1.01 d 3H (6.5)	H-3'	2',3',4',
15'	18.4	1.04 d 3H (6.9)	H-5'	4',5', 6'
16'	11.1	1.67 d 3H (1.1)	-	10',11',12',13'
5O-	56.6	3.88 s 3H	-	5
7O-	56.9	4.00 s 3H	-	7
4'O-	61.7	3.45 s 3H	-	4'
6'O-	56.1	3.17 s 3H	-	12'



Iso-methoxy-stigmatellin A
2

Table S3. Spectroscopic values for stigmatellin C (**3**) acquired in methanol-d₄ at 700 MHz.

Stigmatellin C (3)				
Position	δ_c	δ_H , [m, <i>J</i> (Hz)]	COSY	HMBC
1a	148.1	-	-	-
2	165.5	-	-	-
3	117.3	-	-	-
4	179.7	-	-	-
4a	108.2	-	-	-
5	153.9	-	-	-
6	93.8	6.63 s 1H	-	4a, 5, 7, 8
7	152.6	-	-	-
8	129.6	-	-	-
9	10.0	1.98 s 3H	-	2, 3, 4, 1', 2'
1'	30.5	2.84 m 1H 2.70 m 1H	H-2'	2, 3, 2', 3'
2'	28.3	1.88 m 1H 1.55 m 1H	H-3'	1', 3', 4', 14'
3'	35.5	1.73 m 1H	H-2', H-4', H-14'	2', 14'
4'	88.5	3.11 dd 1H (2.3/9.4)	H-4', H-5'	2', 3', 4'-OCH ₃ , 5', 6', 14', 15'
5'	42.9	1.66 m 1H	H-4'', H-6'', H-15'	4', 15'
6'	82.4	3.88 dd 1H	H-5', H-7'	4', 5', 7', 8', 15', 6'-OCH ₃
7'	133.4	5.60 dd 1H (7.4/15.2)	H-8'	5', 6', 8', 9'
8'	133.8/133.9	6.20 dd 1H (10.5/15.3)	H-7', H-9'	6', 9', 10'
9'	129.6	6.31 ddd 1H (3.3/4.9/7.2/15.4)	H-10'	8', 9', 10'
10'	138.9/139.1	5.81 dd 1H (15.3/20.2)	H-9'	9', 10', 11', 16'
11'	76.3/76.2	-	-	-
12'	74.9/74.8	3.56 s 1H (3.8/6.5)	H-13'	10', 11', 13', 16'
13'	17.8	1.10 dd 3H (6.5/10.5)	-	11', 12', 16'
14'	18.2	1.14 d 3H (6.8)	H-3'	2', 3', 4'
15'	10.3	0.73 d 3H (7.1)	H-5'	4', 5'
16'	23.2	1.24 d 3H (2.1/7.8)	-	9', 10', 11', 12'
5O-	56.7	3.88 s 3H	-	5
7O-	56.9	4.00 s 3H	-	7
4'O-	61.7	3.47 s 3H	-	4'
6'O-	56.6	3.22 s 3H	-	6'

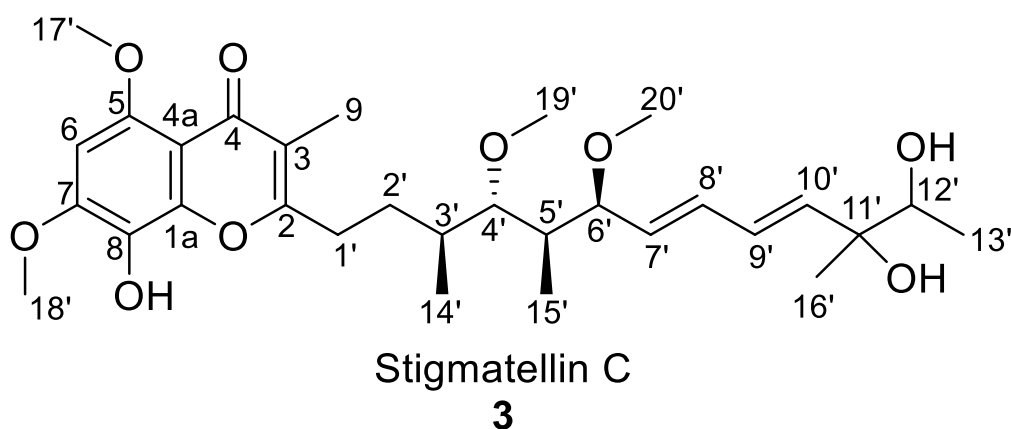
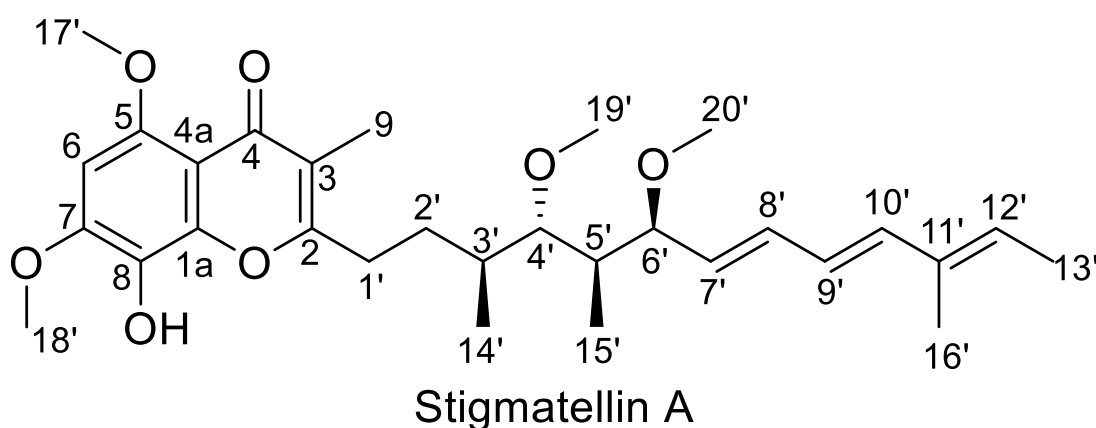


Table S4. Spectroscopic values for stigmatellin A (**4**) acquired in methanol-d₄ at 700 MHz.

Stigmatellin A (4)			
Position	δ_c	δ_H , [m, <i>J</i> (Hz)]	δ_c , type [1]
1a	148.0	-	148.0
2	165.4	-	165.4
3	117.3	-	117.3
4	179.7	-	179.6
4a	108.2	-	108.7
5	153.8	-	154.0
6	93.7	6.59 s 1H	93.8
7	152.5	-	152.6
8	128.9	-	129.1
9	10.0	1.97 s 3H	9.9
1'	30.5	2.83 m 1H 2.67 m 1H	30.6
2'	28.2	1.92 m 1H 1.56 m 1H	28.5
3'	35.5	1.73 m 1H	35.6
4'	88.5	3.20 m 3H	88.8
5'	42.9	1.66 m 1H	43.0
6'	82.4	3.88 m 3H	82.7
7'	132.5	5.57 dd 1H (7.7)	132.5
8'	134.7	6.20 m 1H	134.6
9'	126.4	6.20 m 1H	126.3
10'	138.9	6.20 m 1H	138.9
11'	135.9	-	135.9
12'	128.5	5.57 q 1H (7.7)	128.4
13'	14.0	1.75 s 3H	13.9
14'	18.3	1.14 dd 3H (3.05/6.7)	18.3
15'	10.5	0.74 d 3H (7.0)	10.7
16'	12.1	1.75 s 3H	12.0
17'	56.6	3.87 s 3H	56.8
18'	56.9	3.97 s 3H	57.0
19'	61.7	3.46 s 3H	61.6
20'	56.5	3.20 s 3H	56.5



3. Biosynthetic *in silico* investigation

Table S5. Predicted functions of the encoded proteins by the Stigmatellin BGC from *Vitiosangium cumulatum* MCy10943^T.

Gene	Size (aa)	Deduced function	Closest homolog ¹	Coverage/Identity (%)	Sg a15 homolog
<i>orf1</i>	308	DUF2381 family protein	WP_083682780.1	92/83	---
<i>orf2</i>	393	Serine/Threonine Protein Kinase	WP_204220004.1	99/92	---
<i>orf3</i>	134	Transcriptional regulator	WP_204220003.1	72/86	---
<i>orf4</i>	123	Transcriptional regulator	WP_204220002.1	100/89	---
<i>orf5</i>	458	HNH/ENDO VII superfamily nuclease	WP_204220001.1	93/93	---
<i>orf6</i>	203	Hypothetical protein	WP_203410745.1	96/75	---
<i>orf7</i>	122	Hypothetical protein	MBN1207532.1	82/84	---
<i>orf8</i>	1209	Helicase	WP_149184102.1	97/43	---
<i>orf9</i>	1097	Hypothetical protein	WP_230650848.1	97/32	---
<i>orf10</i>	388	Hypothetical protein	NQT93121.1	96/30	---
<i>orf11</i>	203	Hypothetical protein	WP_095987131.1	99/67	---
<i>stiA</i>	2364	PKS biosynthesis ACP-KS-AT-AT-DH-KR-ACP	AAK57190.1	99/49	99/79
<i>stiB</i>	1588	PKS biosynthesis KS-AT-KR-ACP	WP_203404417.1	97/53	100/82
<i>stiC</i>	1880	PKS biosynthesis KS-AT-DH-KR-ACP	WP_194142736.1	99/47	99/81
<i>stiD</i>	1932	PKS biosynthesis KS-AT-OMT-KR-ACP	WP_075010838.1	98/50	100/83
<i>stiE</i>	1925	PKS biosynthesis KS-AT-OMT-KR-ACP	WP_063796277.1	96/56	100/84
<i>stiF</i>	2212	PKS biosynthesis KS-AT-DH-ER-KR-ACP	BAZ29707.1	98/48	99/84
<i>stiG</i>	1402	PKS biosynthesis KS-AT-DH-ACP	NOT56266.1	87/51	100/81
<i>stiH</i>	1597	PKS biosynthesis KS-AT-DH-ACP	WP_196523766.1	95/48	99/79
<i>stiJ1</i>	1045	PKS biosynthesis KS-AT-ACP	MBD1836177.1	87/58	99/84
<i>stiJ2</i>	180	PKS biosynthesis	MBW4628907.1	99/28	99/78
<i>stiK</i>	256	PKS biosynthesis tailoring <i>O</i> -Methyltransferase	MBA2429587.1	100/51	100/85
<i>stiL1</i>	306	PKS biosynthesis tailoring Cytochrome P450 enzyme	WP_104977779.1	79/43	82/82
<i>stiL2</i>	230	PKS biosynthesis tailoring Cytochrome P450 enzyme	CTS25513.1	79/43	82/82
<i>orf12</i>	374	Transport	WP_108074850.1	100/95	---
<i>orf13</i>	911	Transport	WP_108074851.1	99/93	---
<i>orf14</i>	345	Transport	WP_108074852.1	95/88	---
<i>orf15</i>	530	Transport	WP_108074853.1	100/89	---
<i>orf16</i>	701	Glycogen debranching enzyme	MBC7855611.1	95/62	---
<i>orf17</i>	365	ATP-dependent 6-phosphofructokinase	WP_043407704.1	100/96	---
<i>orf18</i>	326	Glucokinase	WP_108074855.1	95/91	---
<i>orf19</i>	359	D-arabitol-phosphate dehydrogenase	WP_233262020.1	100/93	---
<i>orf20</i>	486	Pyruvate Kinase	WP_108074856.1	100/92	---
<i>orf21</i>	350	Hydroxyacid dehydrogenase	PTL78120.1	100/93	---
<i>orf22</i>	124	Hypothetical protein	WP_108074858.1	85/91	---

¹For *stiA*–*stiL2* the second closest homolog was denoted.

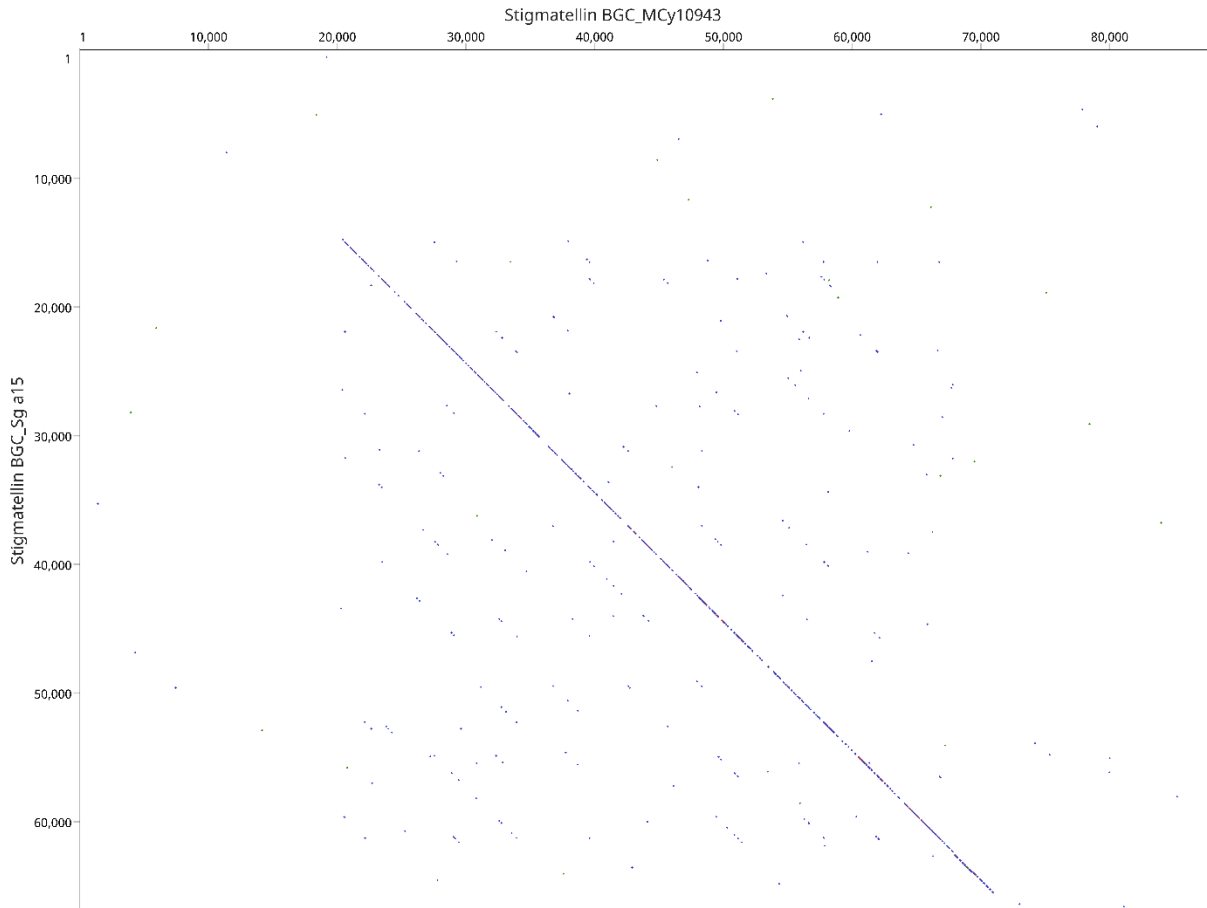


Figure S15. Dotplot of the entire herein identified Stigmatellin BGC from *Vitiosangium cumulatum* MCy10943^T (GenBank: ON210143, 87854 bp) and the previously characterized BGC from Sg a15 (MIBiG: BGC0000153, 66808 bp). The blue diagonal line indicates the conserved genetic region responsible for the biosynthesis of stigmatellin in both producer strains (*stiA–stiL*), while the surrounding area is different and does not show similarity to each other (no visible lines indicate any similarity between *orf1–22* (MCy10943) and *orf1–8* (Sg a15)).

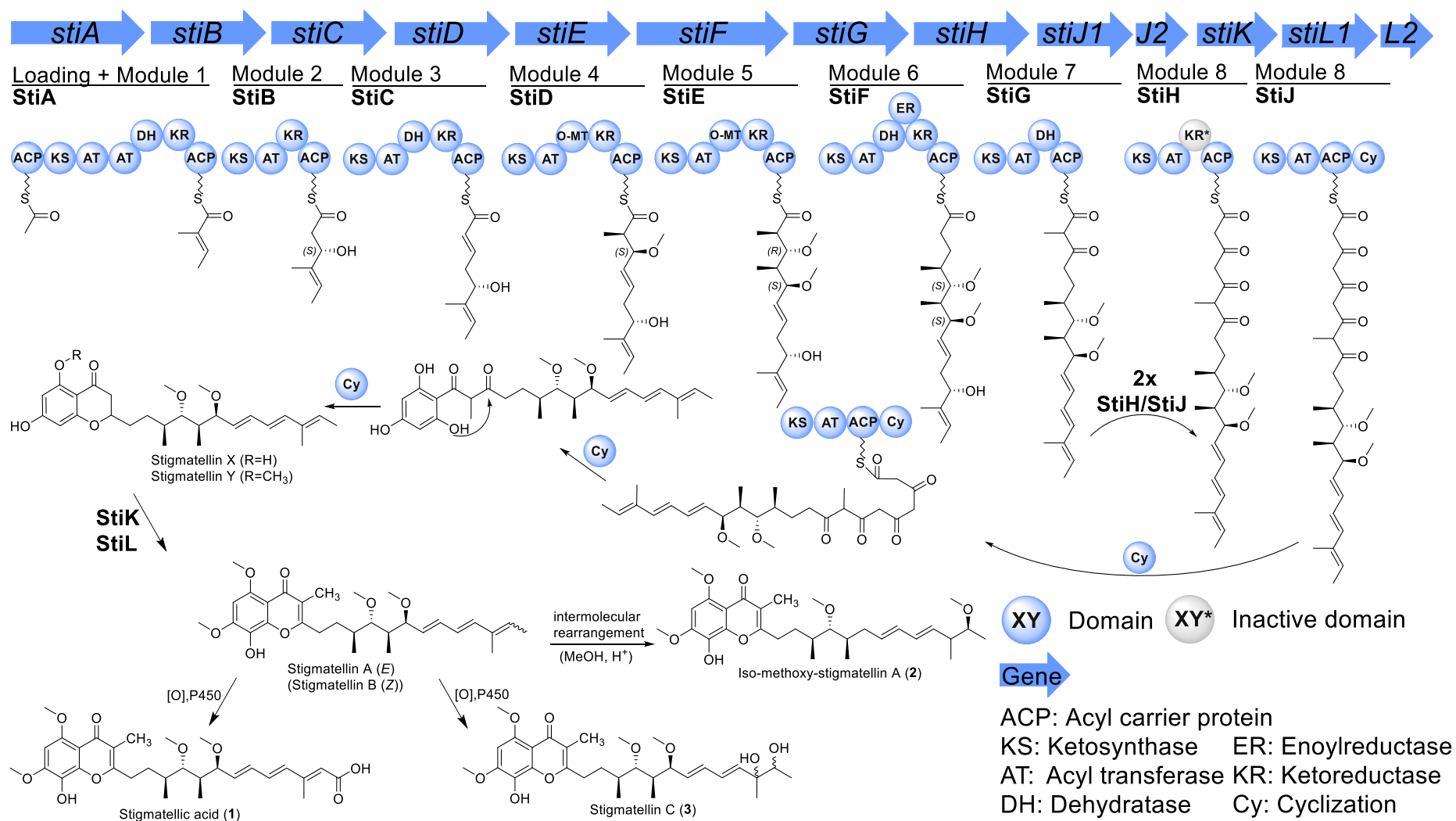


Figure S16. Genetic organization of the Stigmatellin BGC from *Vitosangium cumulatum* MCy10943^T and the proposed model of the biosynthesis leading to 1–3. The stereochemical assignment of the linear biosynthetic intermediates bound to the assembly line was assigned based on the absolute configuration of 1–3. Scheme adapted from Gaitatzis et al. [1] and Wenzel et al. [2].

Table S6 Alignment of KR domain sequences from the stigmatellin biosynthesis (MCy10943) and comparison of predicted and observed product stereochemistry. Influential residues in the sequence are shown in bold letters. Since the predicted stereospecificity of the KR domains involved in the stigmatellin biosynthesis in the myxobacterial strain *V. cumulatum* MCy10943^T is – according to previously identified sequence motifs within KR domains [3] – identical to the homologs in the myxobacterial strain *S. aurantiaca* Sg a15 (**Table S7**), the absolute configuration of **1** and **3** might resemble the absolute configuration of **4**.

Gene	Module	Loop region	Catalytic region	KR type	Pred.	Obs.
<i>stiA</i>	1	HAAGLL DDG TVLQL	SSSASLVGMPGQGN Y AAANA	B	active (C ^S)	C=C (<i>E</i>)
<i>stiB</i>	2	HAAGV LDDG VLLRQ	SSMASALGSRGQGN Y AAANA	B	C ^S -OH	C=C (<i>E</i>)
<i>stiC</i>	3	HAAGVVQDGALLRQ	SSAASLLGPRGQGN Y AAGNA	?	active	C=C (<i>E</i>)
<i>stiD</i>	4	HAAGVAHPRSLVEL	SSGSALMSSPMLGG Y AAANS	?	active	C ^S -OH
<i>stiE</i>	5	HSAV LDDG VLLQ Q	SSLASMLGAPGQGN Y TAAGA	B1	active	C ^S -OH
<i>stiF</i>	6	HSAGV LDDG VLRQ	SSVASLFGSASQGN Y AAANAF	B	active (C ^S)	CH ₂
<i>stiH</i>	7	HTGGPWTVRASREL	SSVASVWGS G LSHHAAAH	---	inactive	C=O

Table S7 Alignment of KR domain sequences from the stigmatellin biosynthesis (Sg a15) and comparison of predicted and observed product stereochemistry. Influential residues in the sequence are shown in bold letters.

Gene	Module	Loop region	Catalytic region	KR type	Pred.	Obs.
<i>stiA</i>	1	HAAGLL DDG TVLQL	SSAASLVGIPGQGN Y AAGNA	B	active (C ^S)	C=C (<i>E</i>)
<i>stiB</i>	2	HAAGV LDDG VLRQ	SSMASALGSRGQGN Y AAANA	B	C ^S -OH	C=C (<i>E</i>)
<i>stiC</i>	3	HAAGVVQDGALLRQ	SSAASLLGPRGQGN Y AAGNA	?	active	C=C (<i>E</i>)
<i>stiD</i>	4	HAAGVANPKPLADL	SSGSALMSSP L GG Y AAANAF	?	active	C ^S -OH
<i>stiE</i>	5	HSAV LDDG VLLK Q	SSLASMLGAPGQGN Y TAAGA	B1	active	C ^S -OH
<i>stiF</i>	6	HSAGV LDDG VLRQ	SSI A S M FGSASQGN Y AAANAF	B	active (C ^S)	CH ₂
<i>stiH</i>	7	HAGGAWTPRASRD	SSVASVWGS G LSHHAAAH	---	inactive	C=O

4. ^1H and ^{13}C NMR spectra

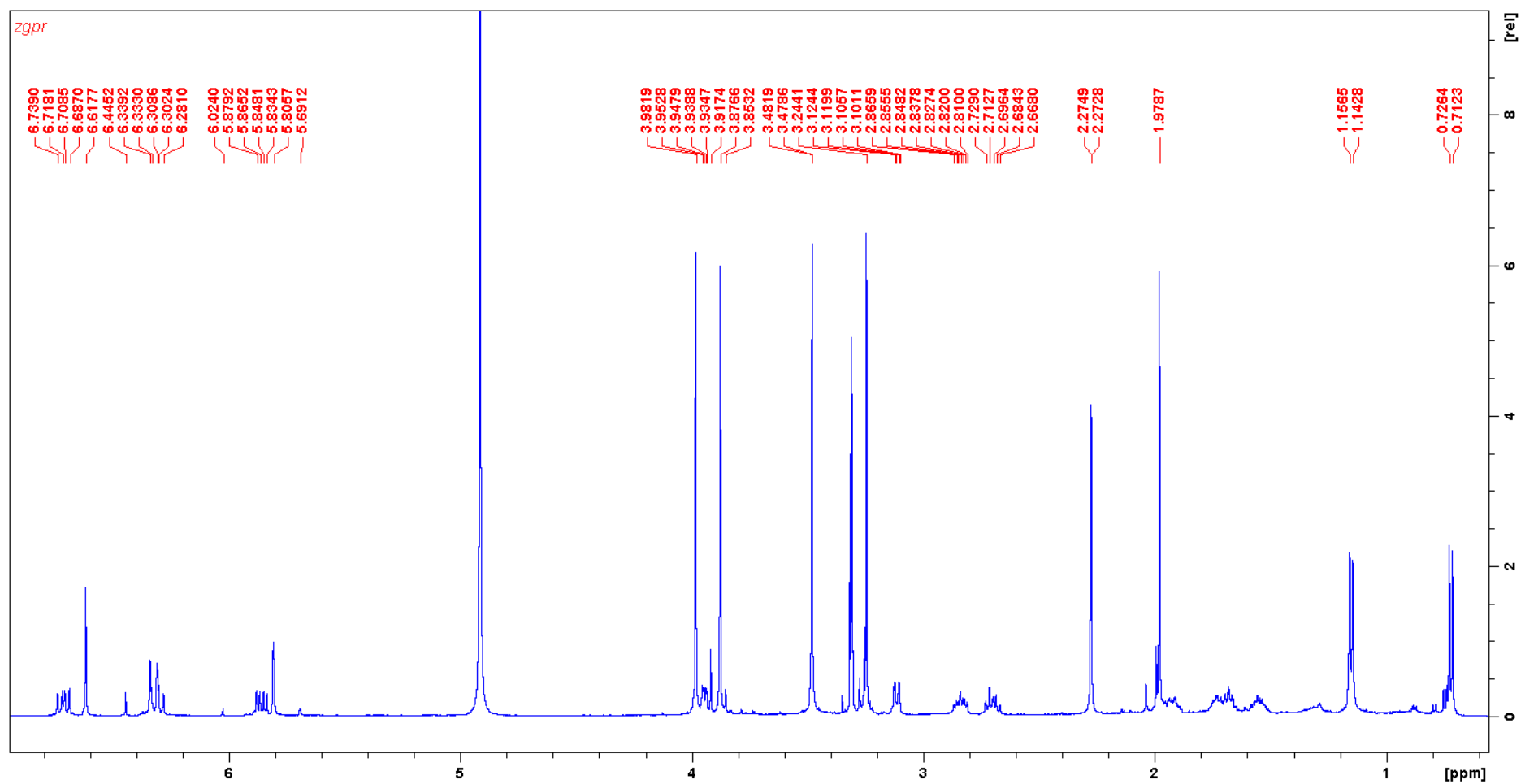


Figure S17. ^1H NMR spectrum of stigmatelic acid (1) in methanol- d_4 .

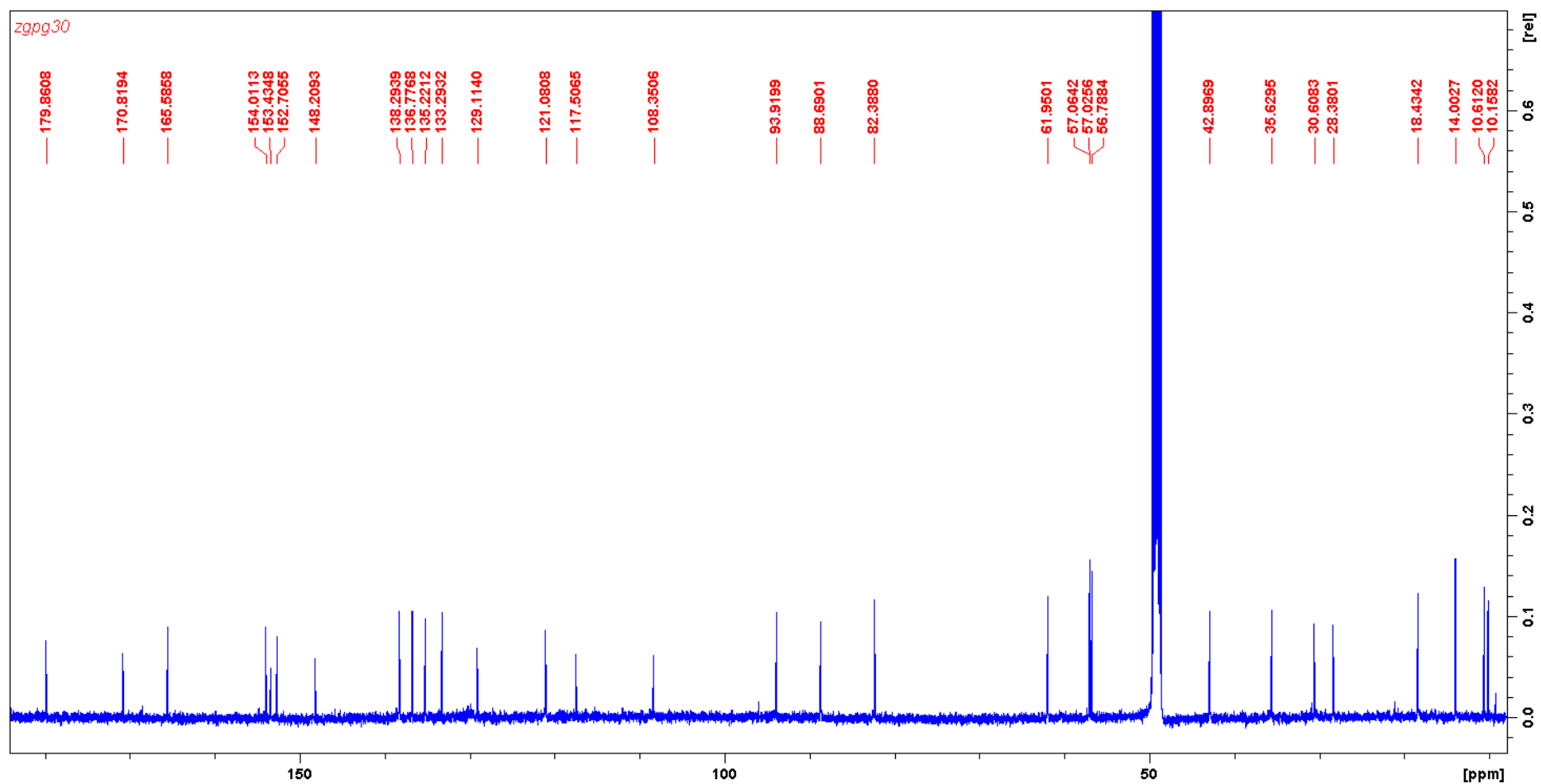


Figure S18. ^{13}C NMR spectrum of stigmatelic acid (1) in methanol- d_4 .

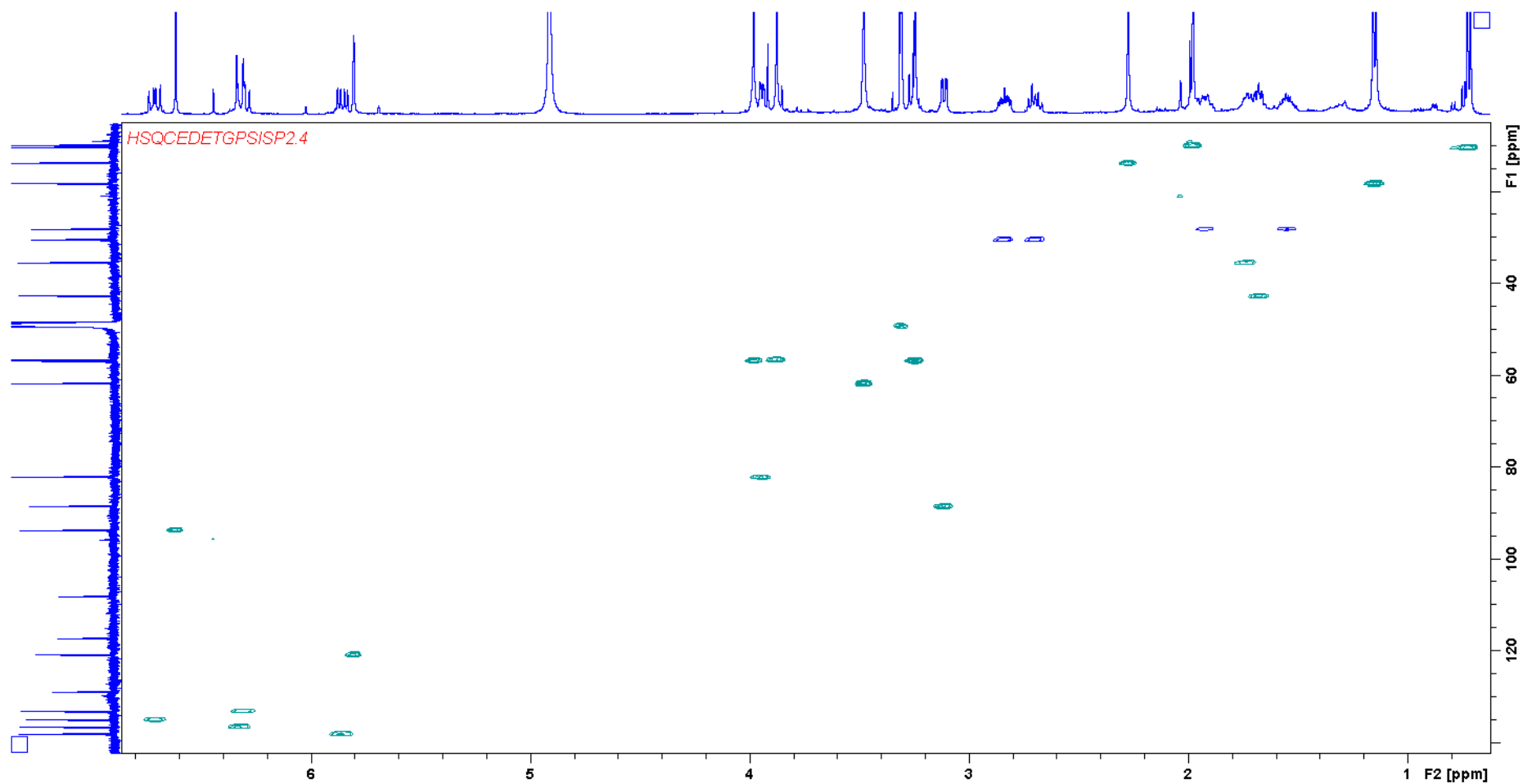


Figure S19. *HSQC* spectrum of stigmatellic acid (**1**) in methanol- d_4 .

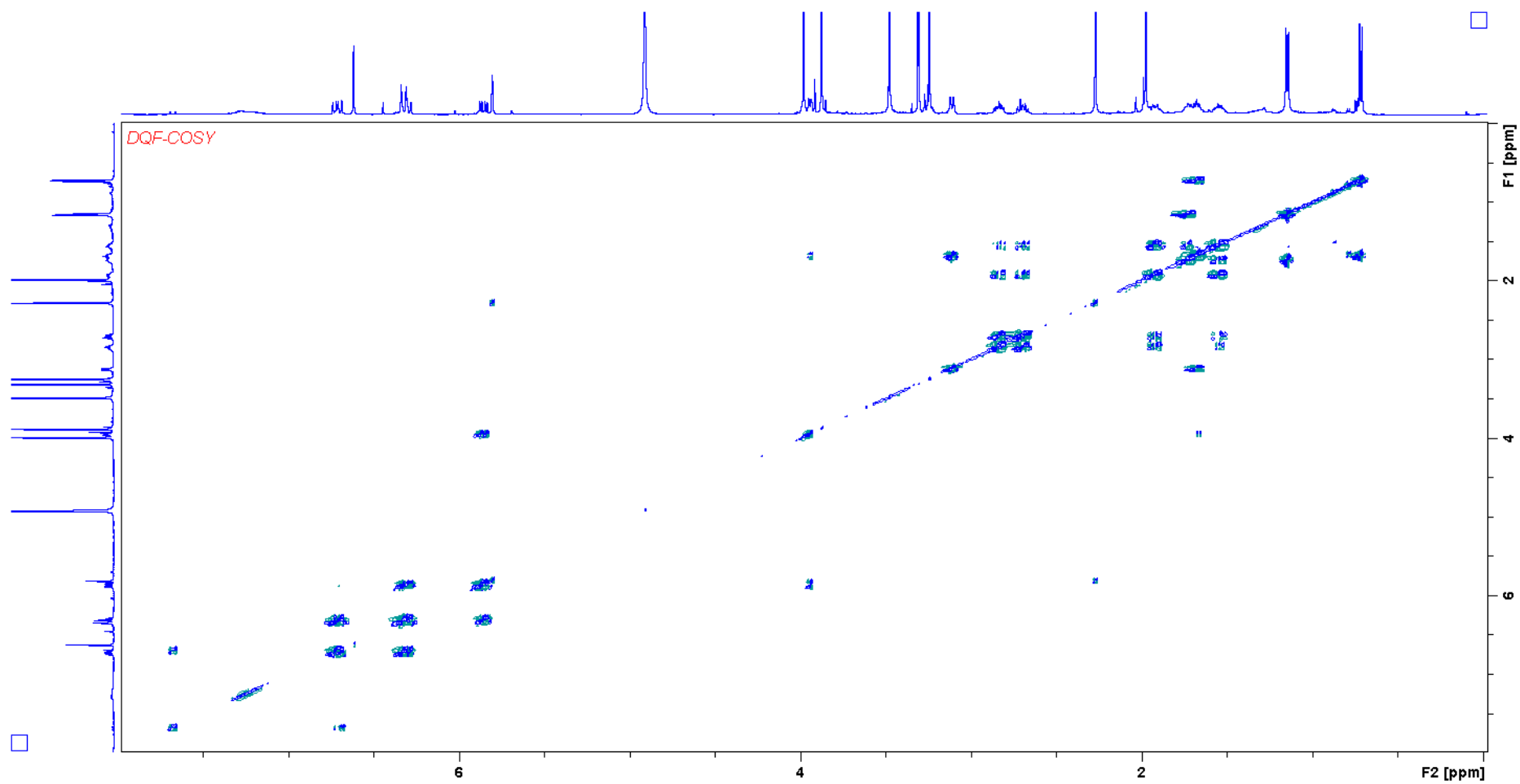


Figure S20. *DQF-COSY* spectrum of stigmatellic acid (**1**) in methanol- d_4 .

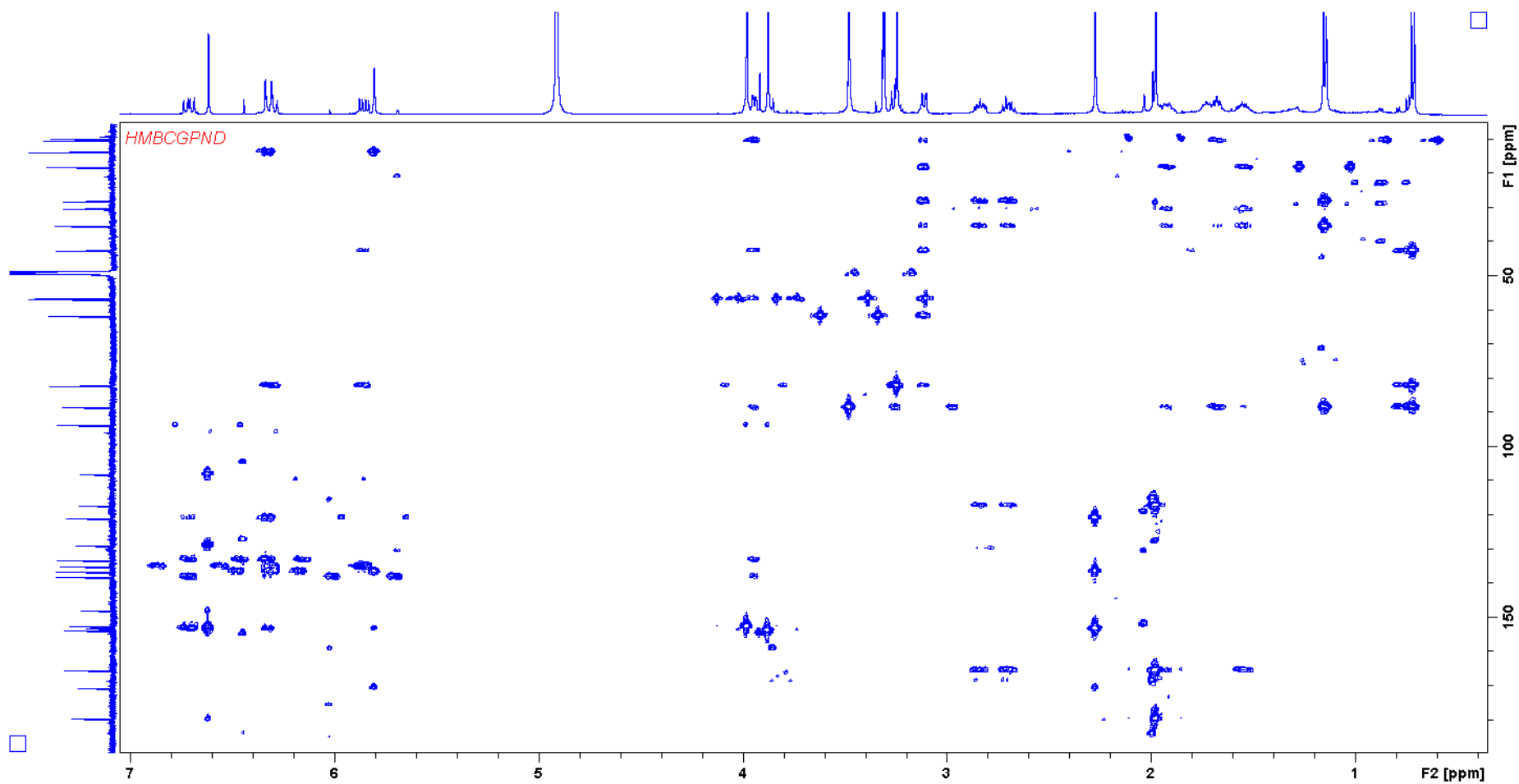


Figure S21. *HMBC* spectrum of stigmatelic acid (**1**) in methanol- d_4

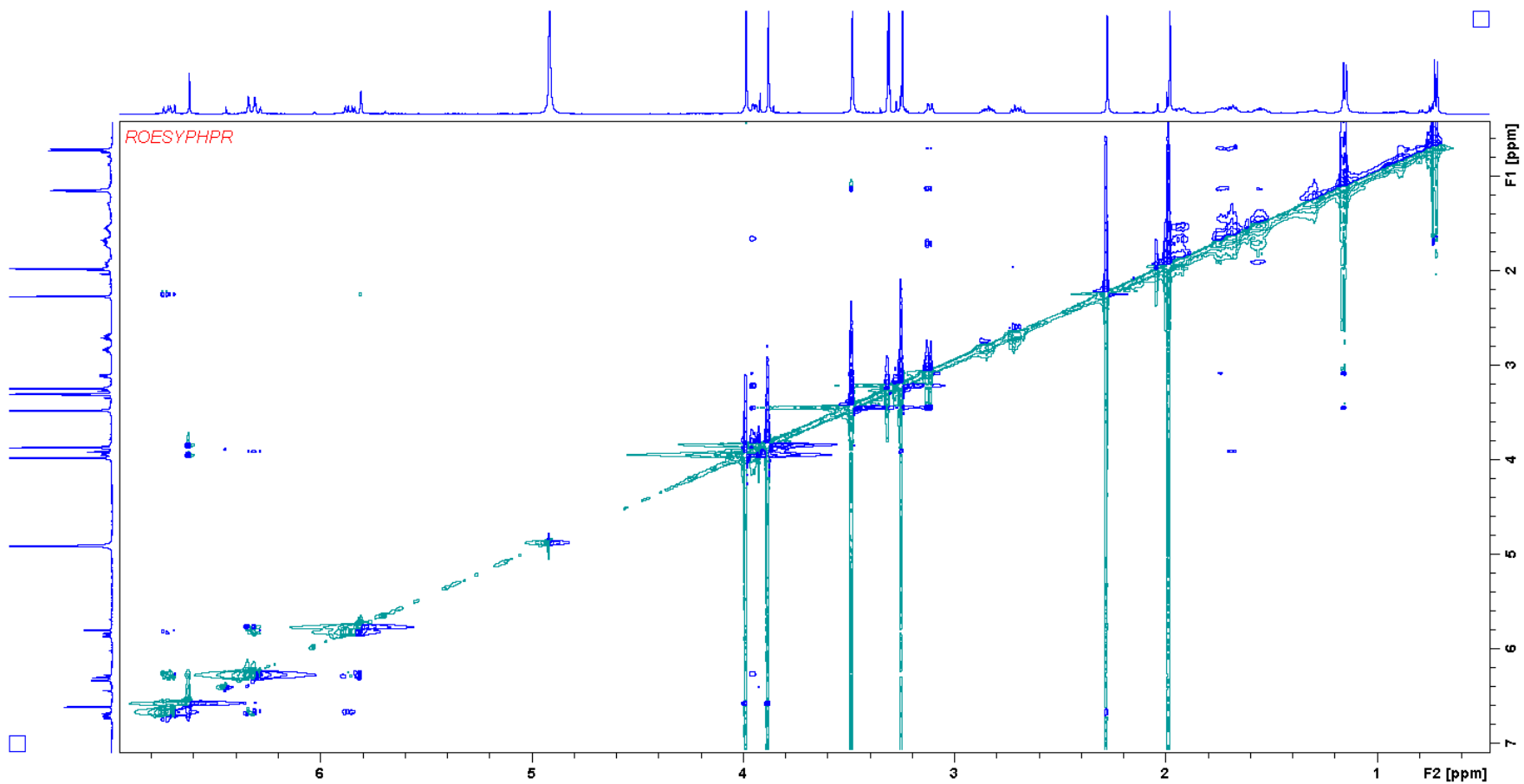


Figure S22. ROESY spectrum of stigmatellic acid (**1**) in Methanol- d_4

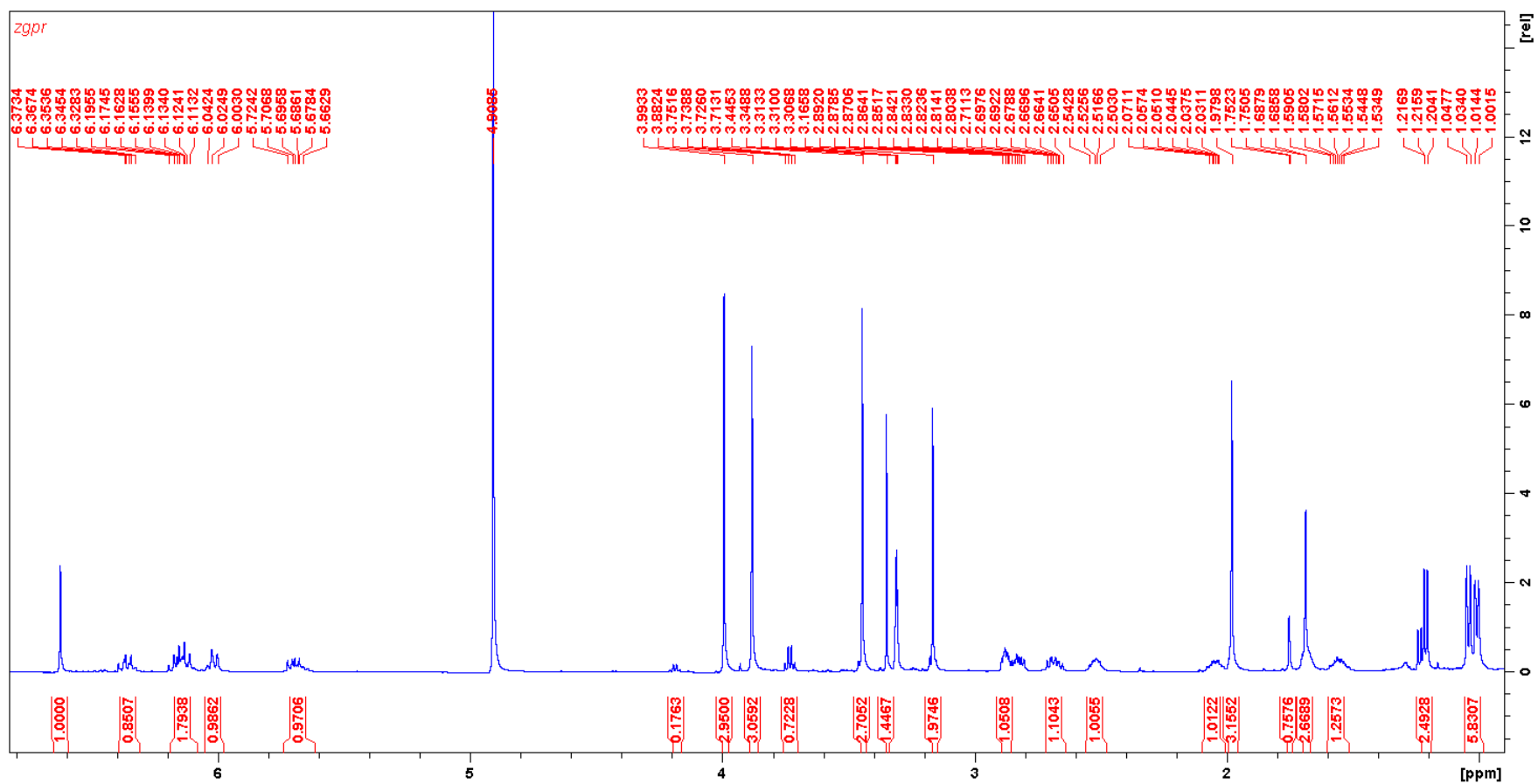


Figure 23: ¹H NMR of iso-methoxy stigmatellin A in methanol-d₄.

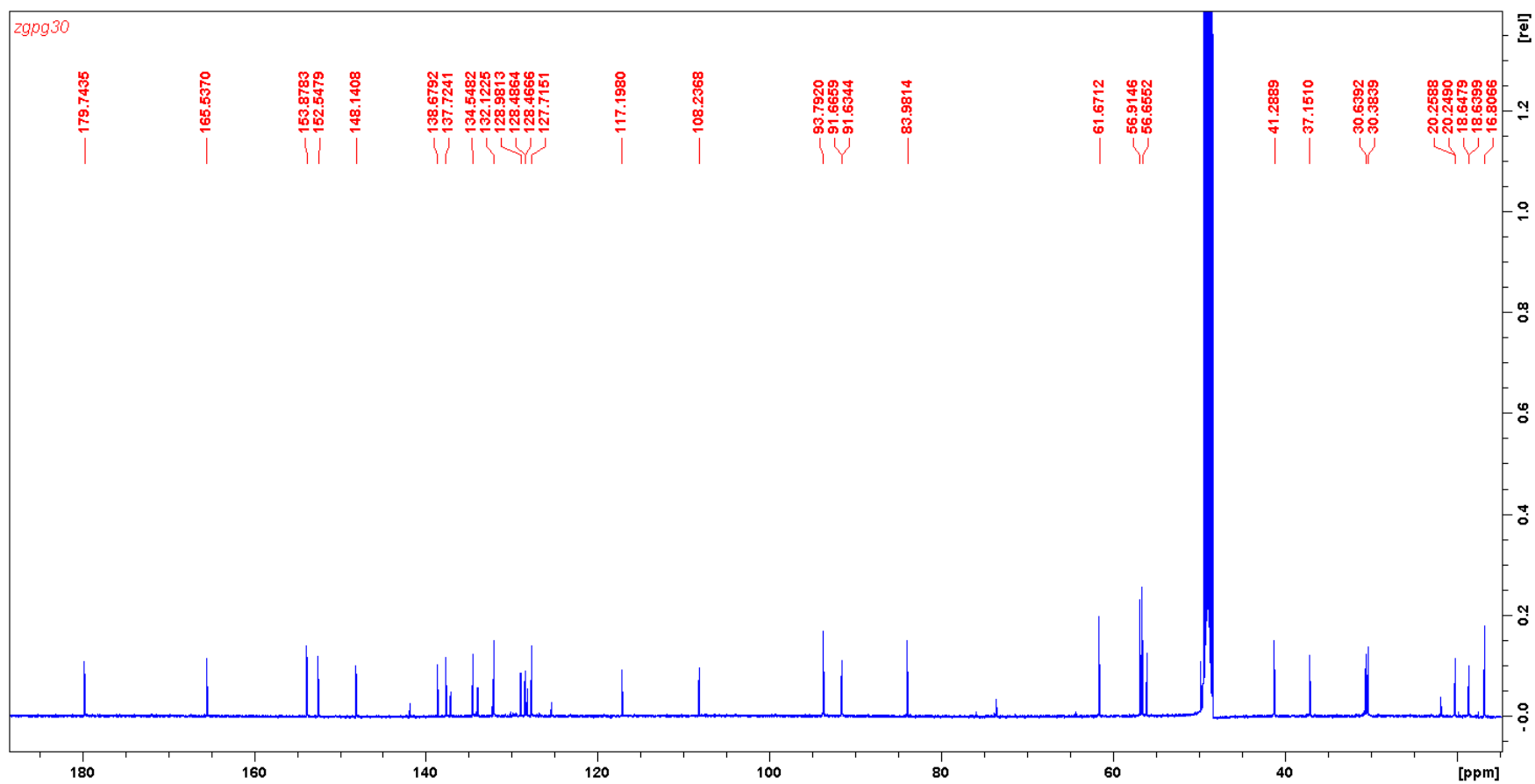


Figure 24: ^{13}C NMR of iso-methoxy stigmatellin A in methanol- d_4 .

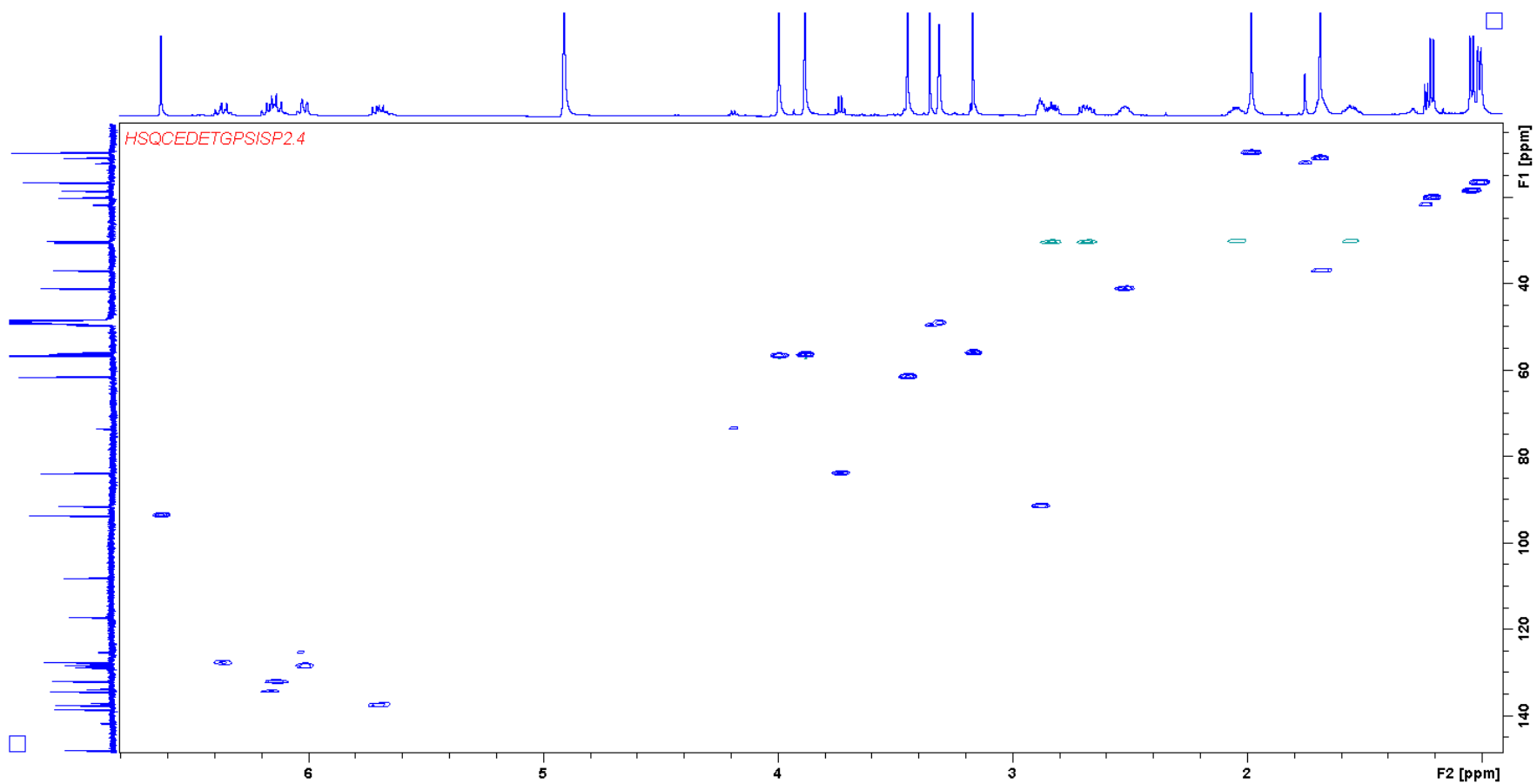


Figure 25: HSQC spectrum of iso-methoxy stigmatellin A in methanol-d₄.

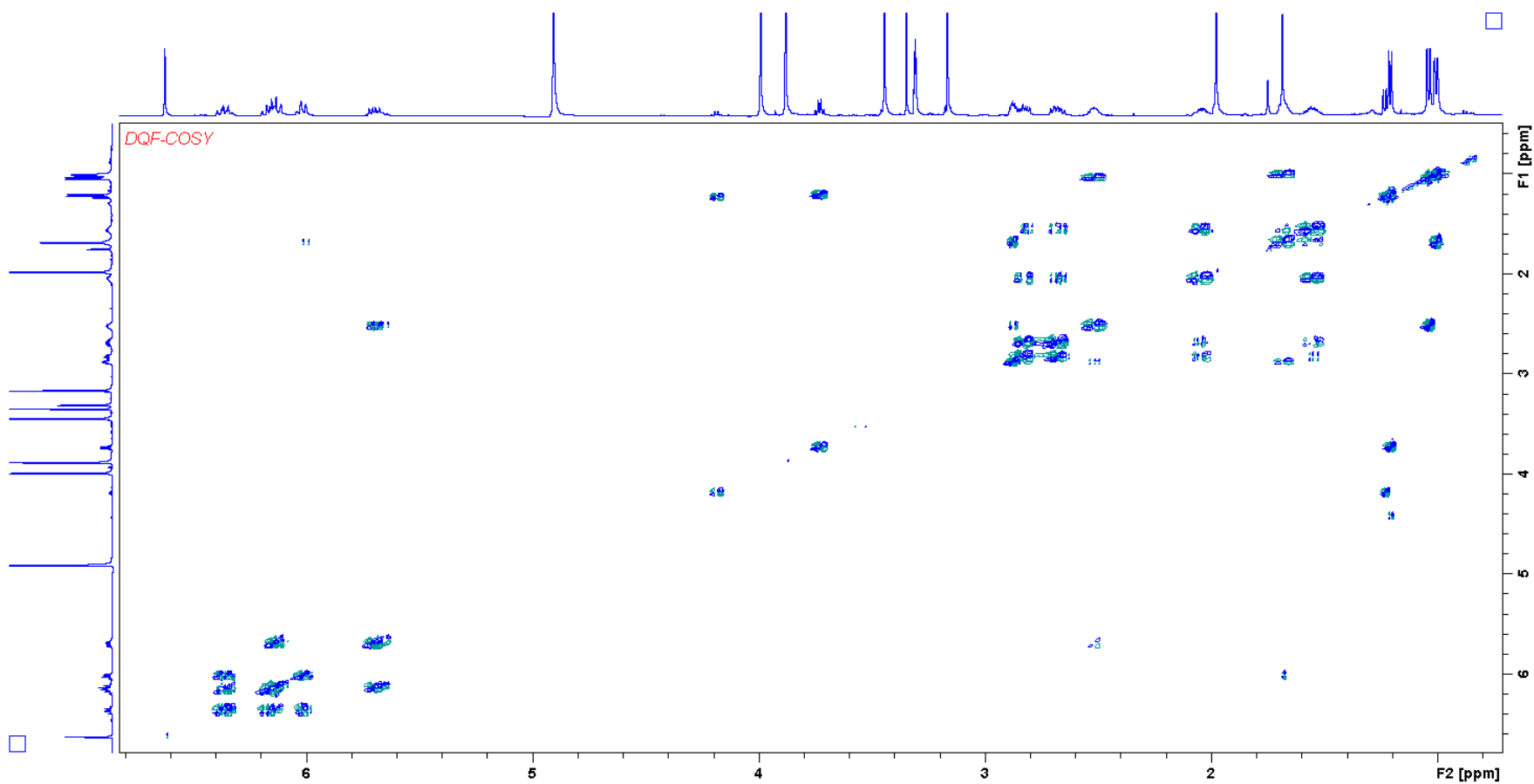


Figure 26: DQF-COSY spectrum of iso-methoxy stigmatellin A in methanol- d_4 .

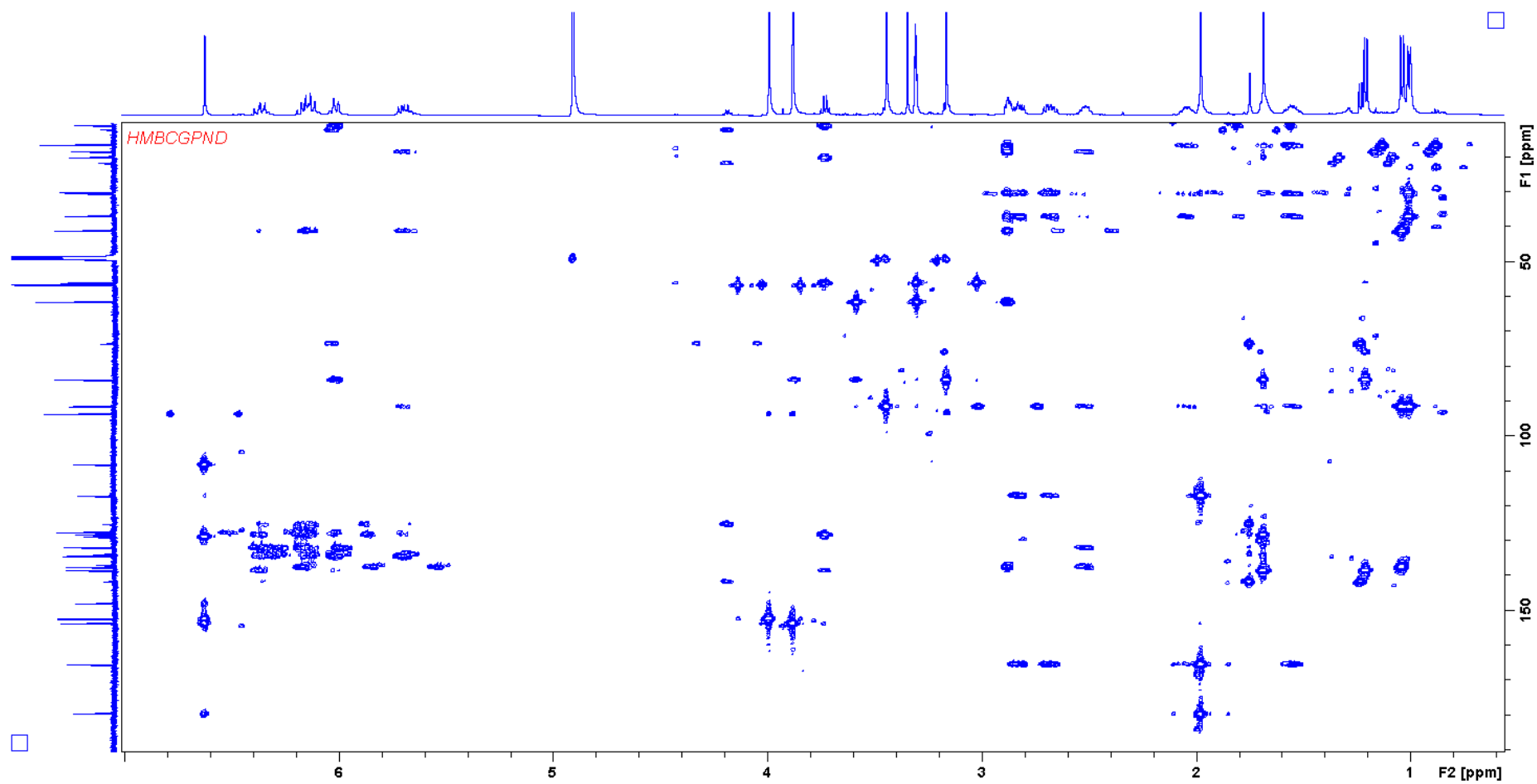


Figure 27: HMBC spectrum of iso-methoxy stigmatellin A in methanol-d₄.

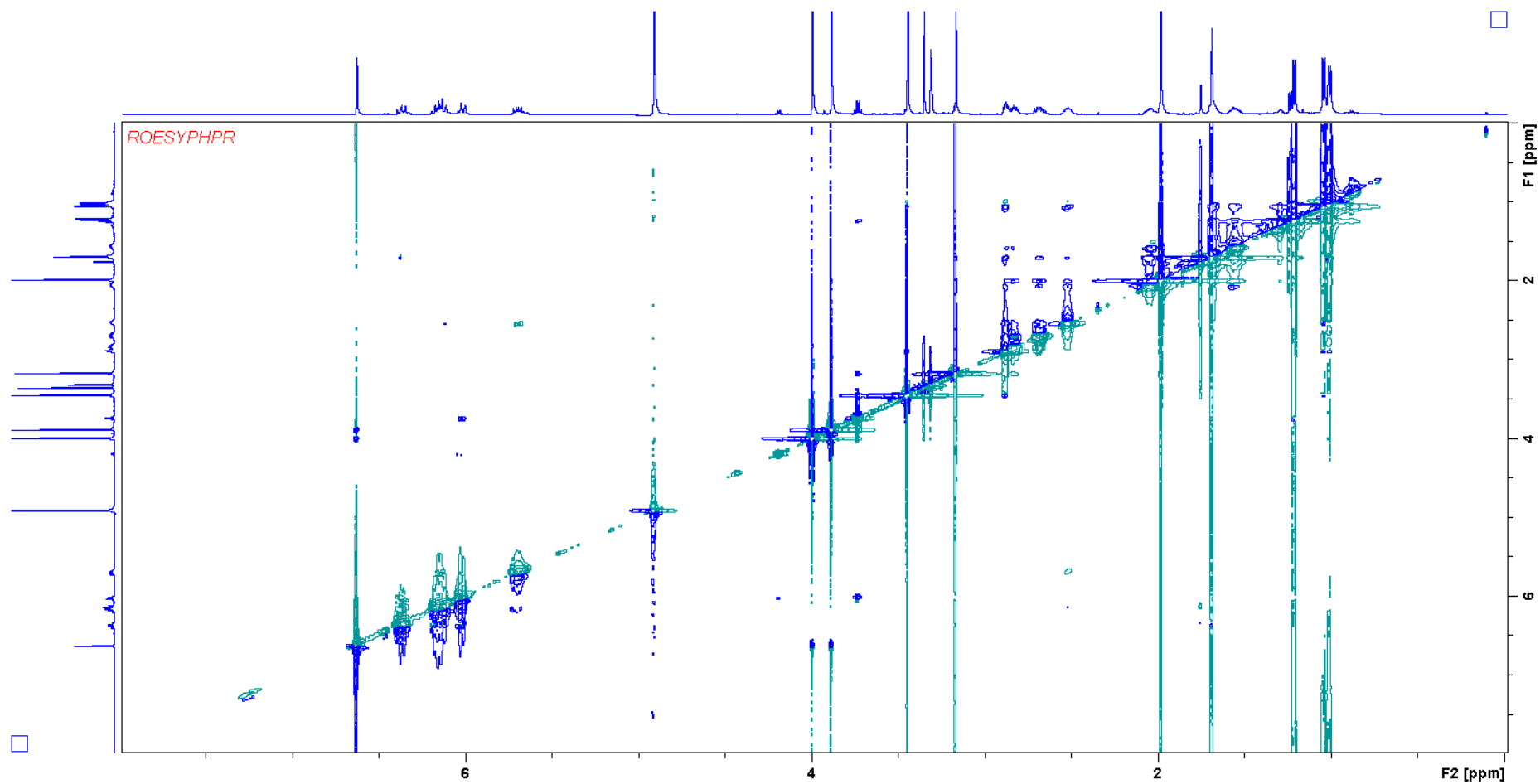


Figure 28: ROESY spectrum of iso.methoxy stigmatellin A in methanol-d₄.

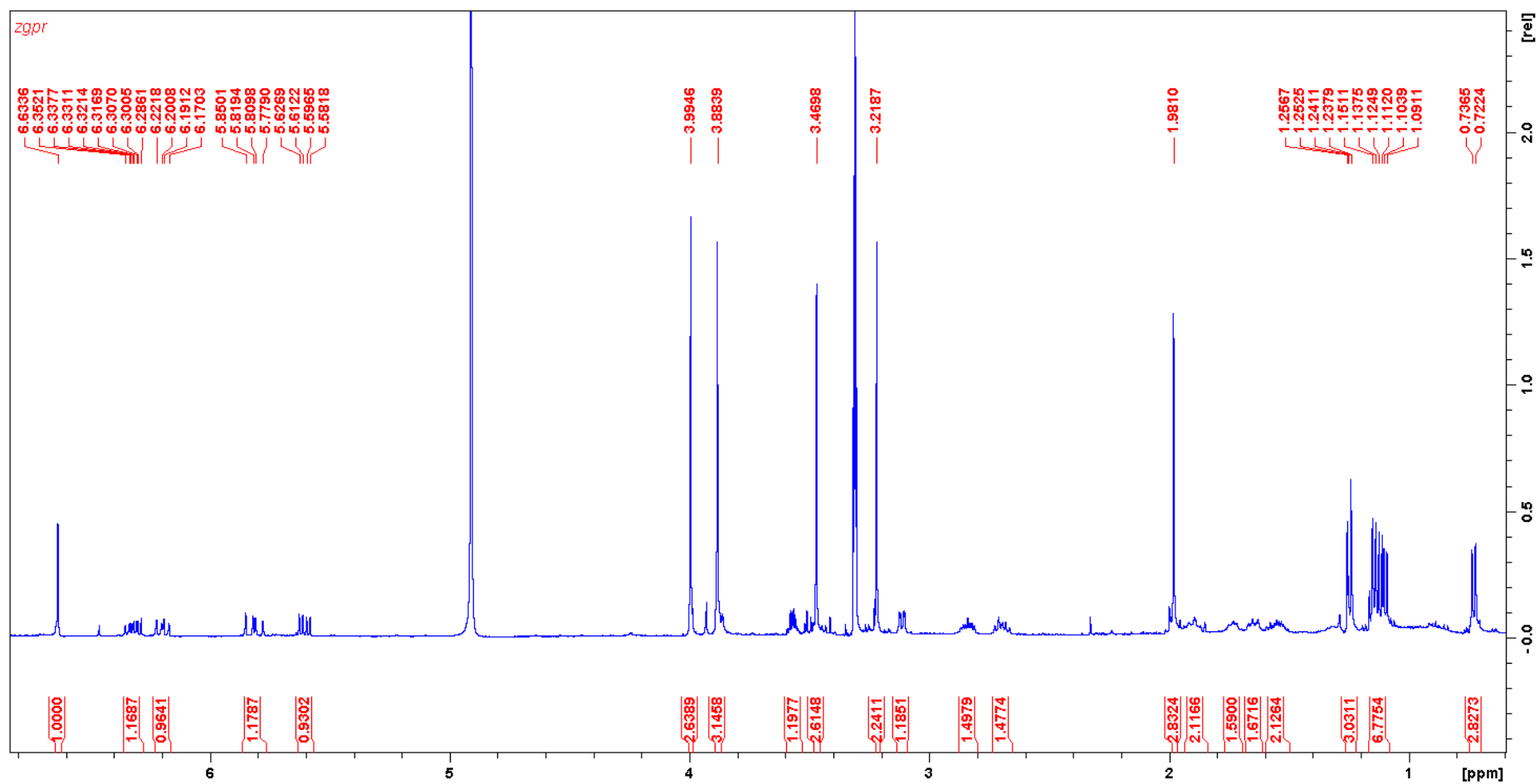


Figure S29. ¹H NMR spectrum stigmatellin C (3) in methanol-d₄.

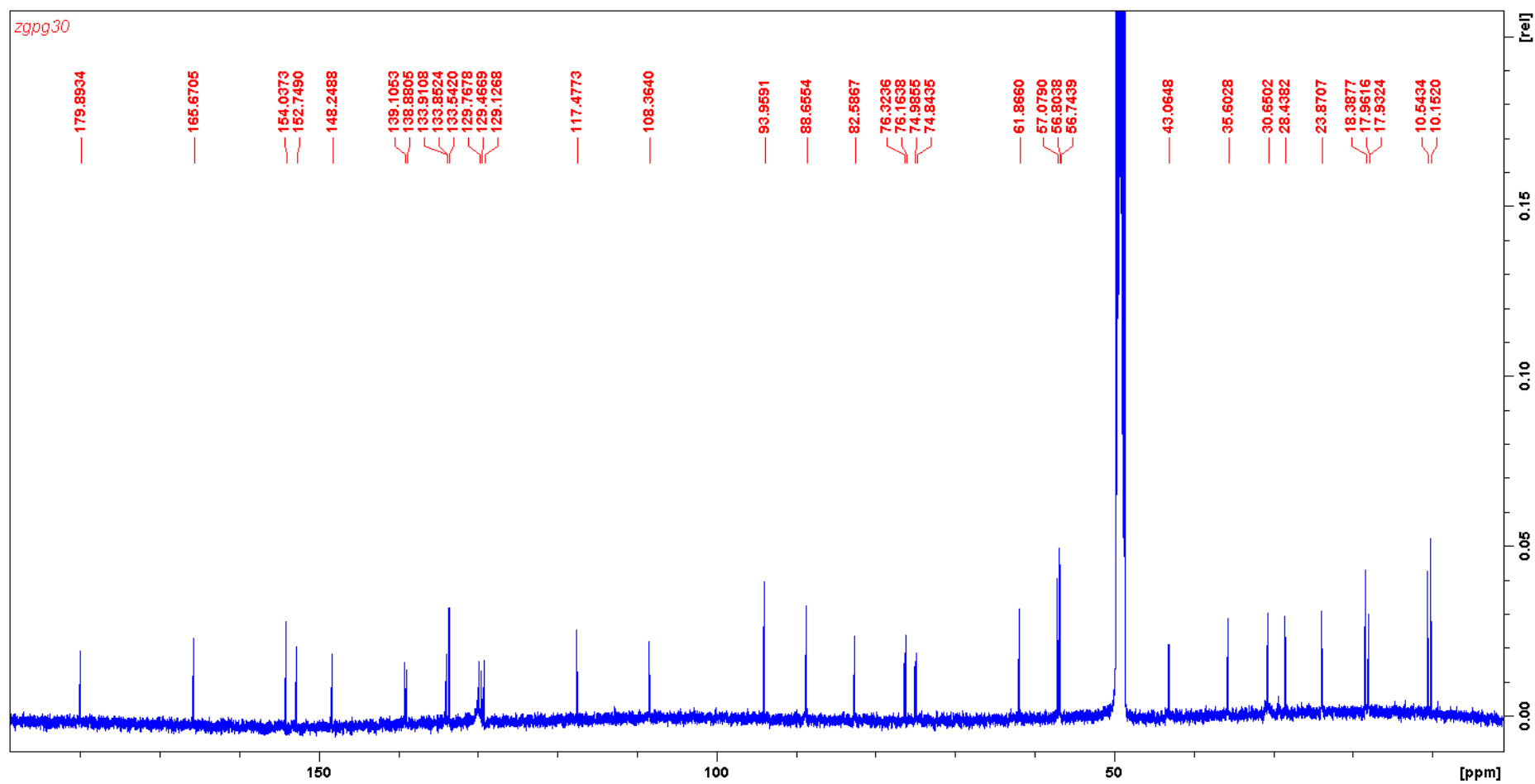


Figure S30. ^{13}C NMR spectrum of stigmatellin C (3) in methanol- d_4 .

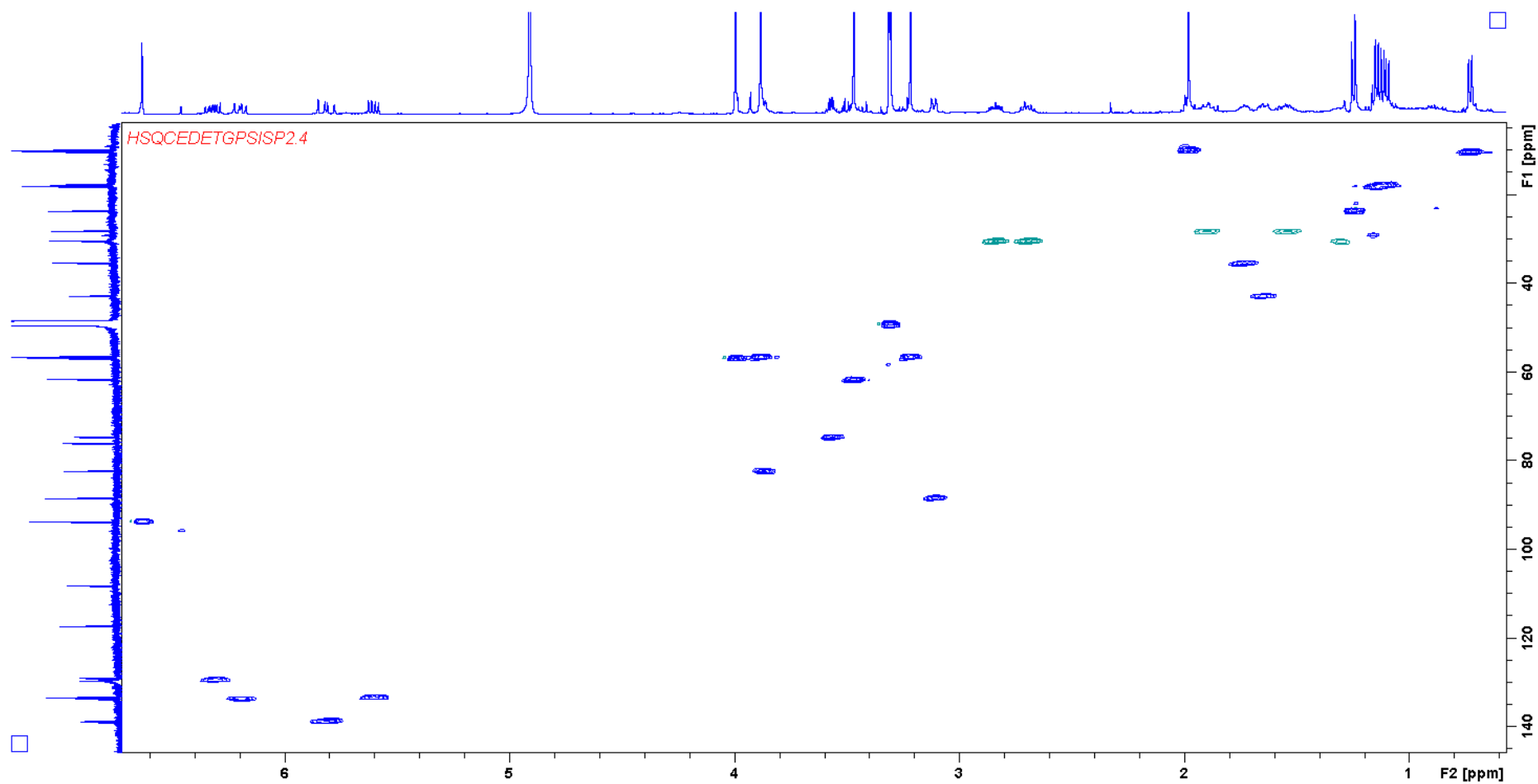


Figure S31. *HSQC* spectrum of Stigmatellin C (**3**) in methanol- d_4 .

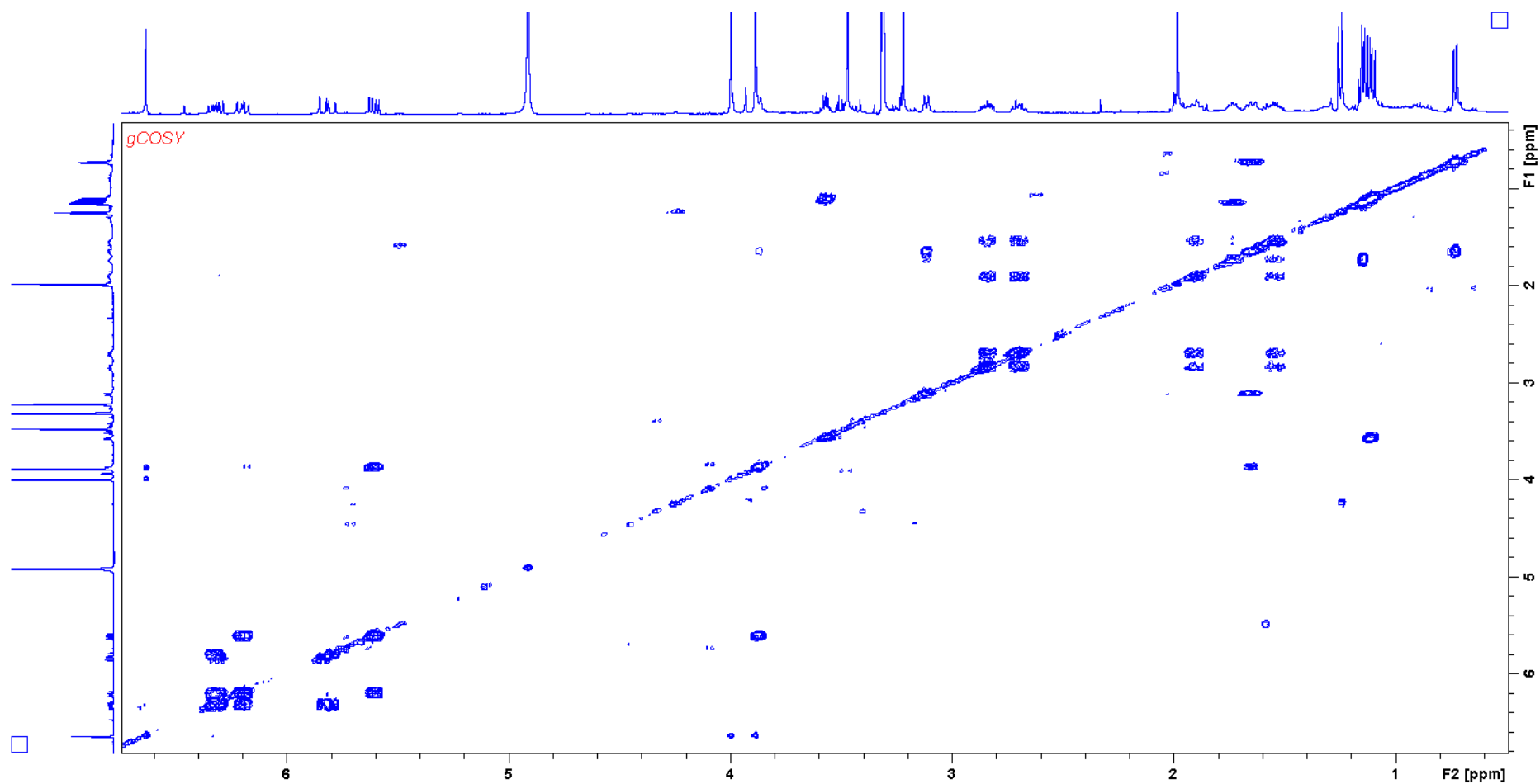


Figure S32. *g*-COSY spectrum of stigmatellin C (3) in methanol- d_4 .

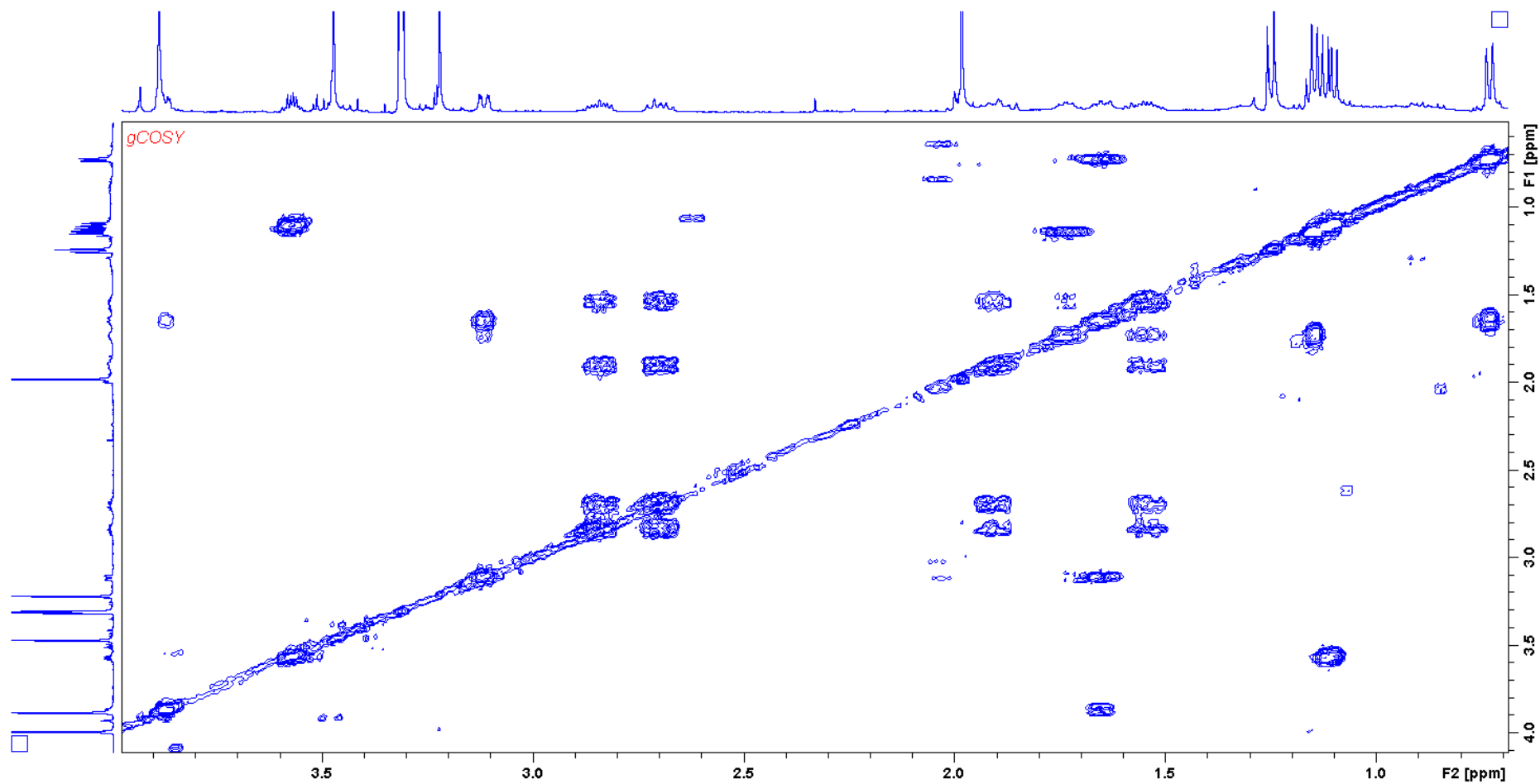


Figure S33: ^1H - ^1H *g*-COSY spectrum (expanded) of stigmatellin C (**3**) in methanol- d_4 .

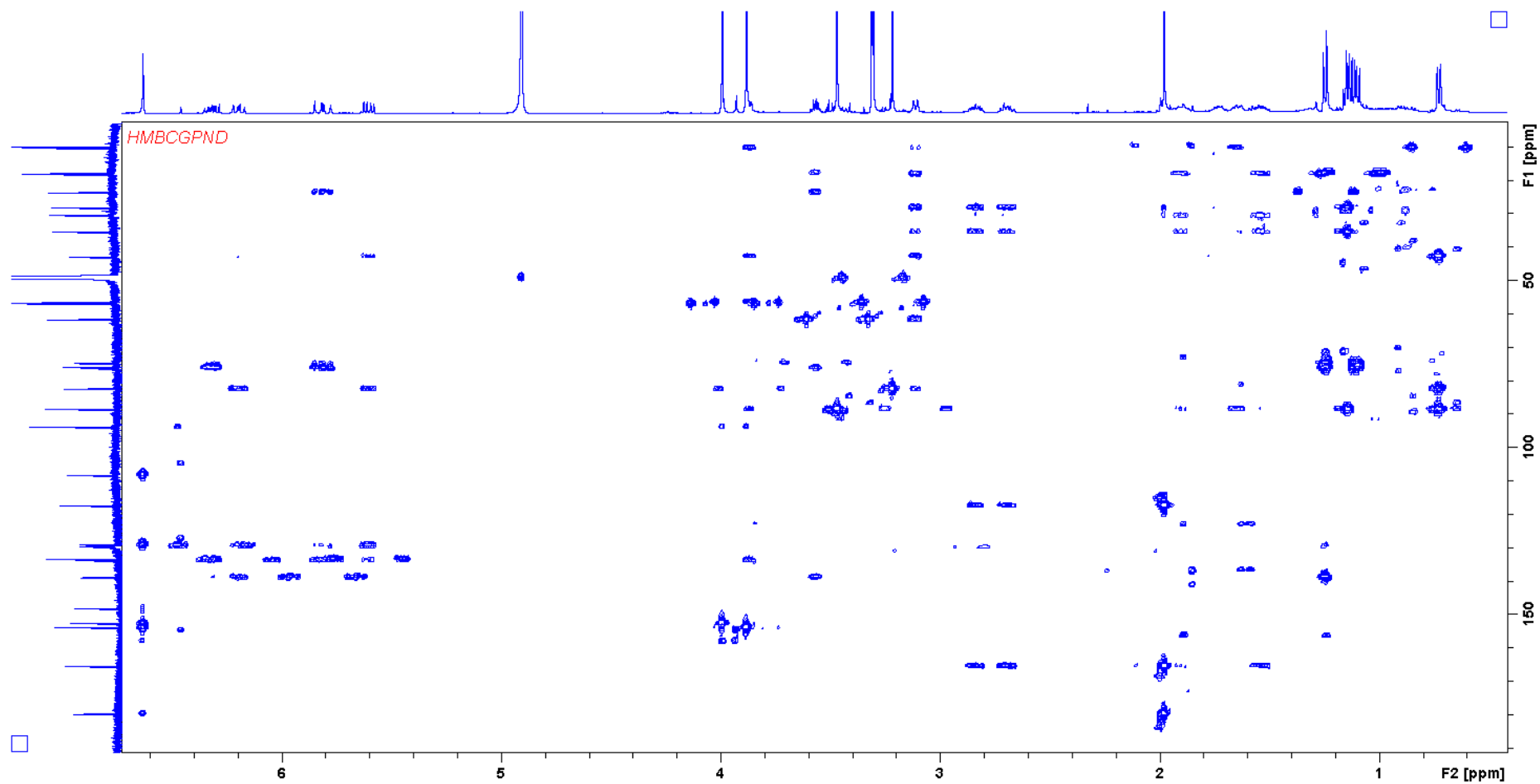


Figure S34. ^1H - ^{13}C *HMBC* spectrum of stigmatellin C (**3**) in methanol- d_4 .

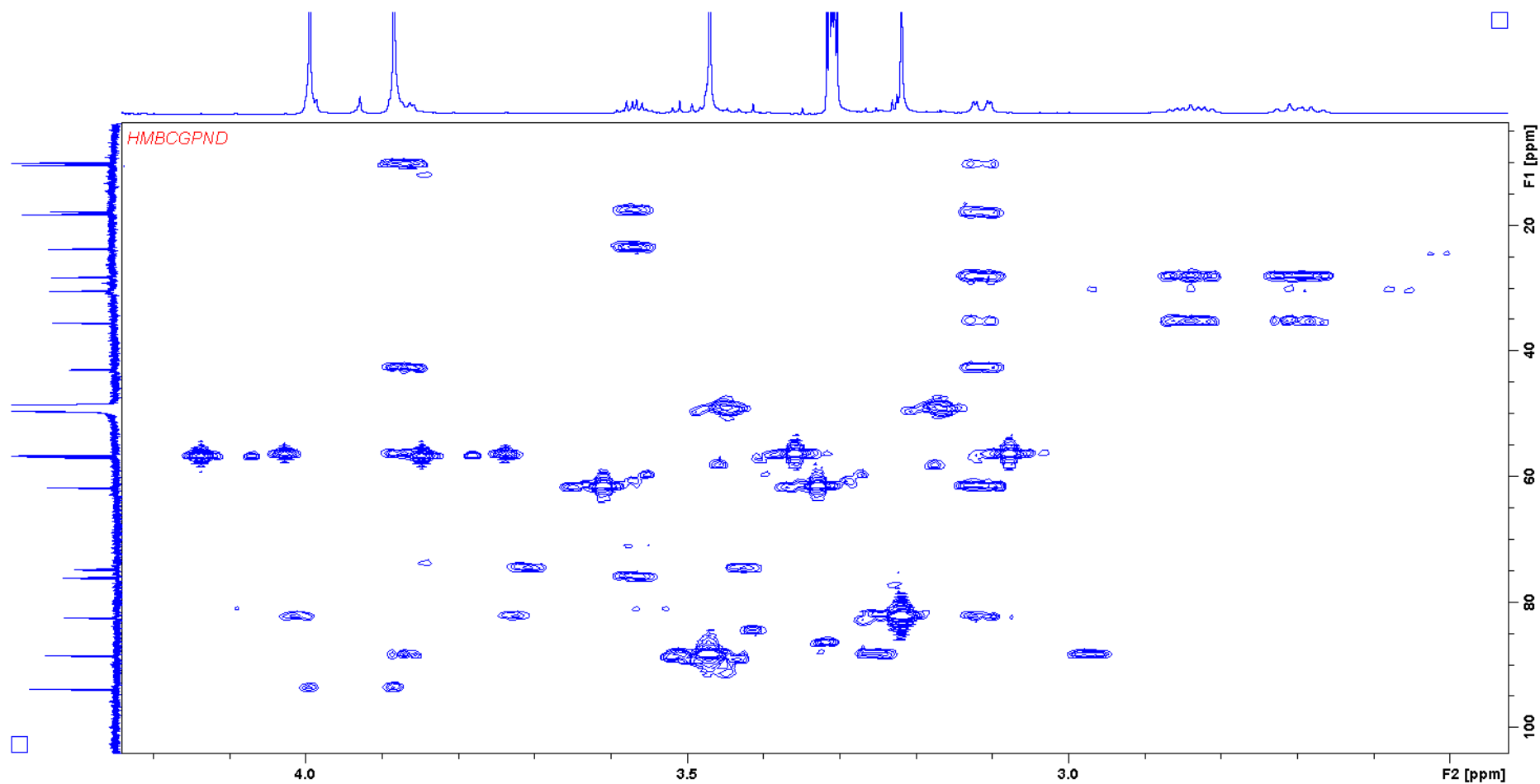


Figure S35 ^1H - ^{13}C HMBC spectrum (expanded) of stigmatellin C (**3**) in methanol- d_4 .

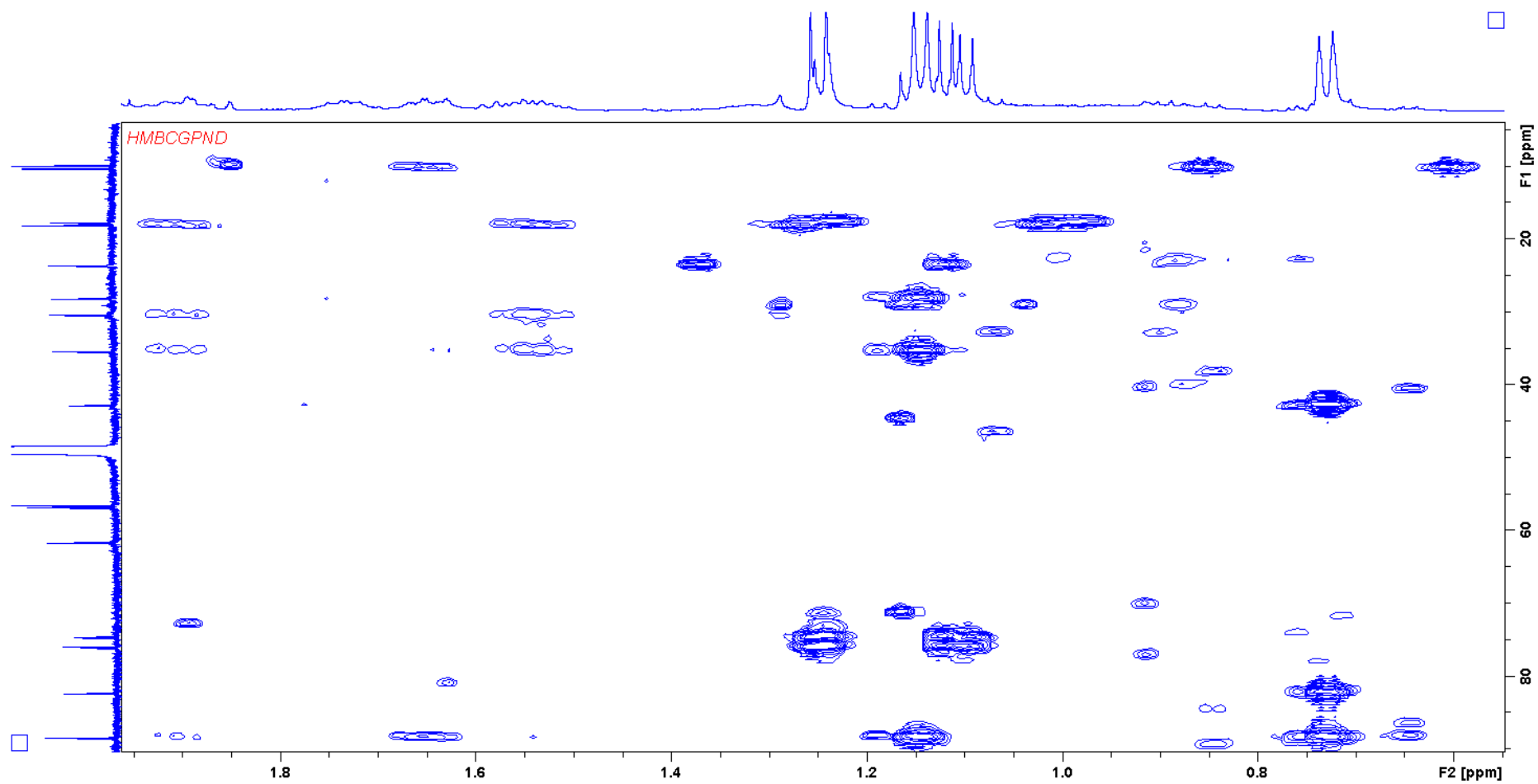


Figure S36 ^1H - ^{13}C HMBC spectrum (expanded) of stigmatellin C (3) in methanol- d_4 .

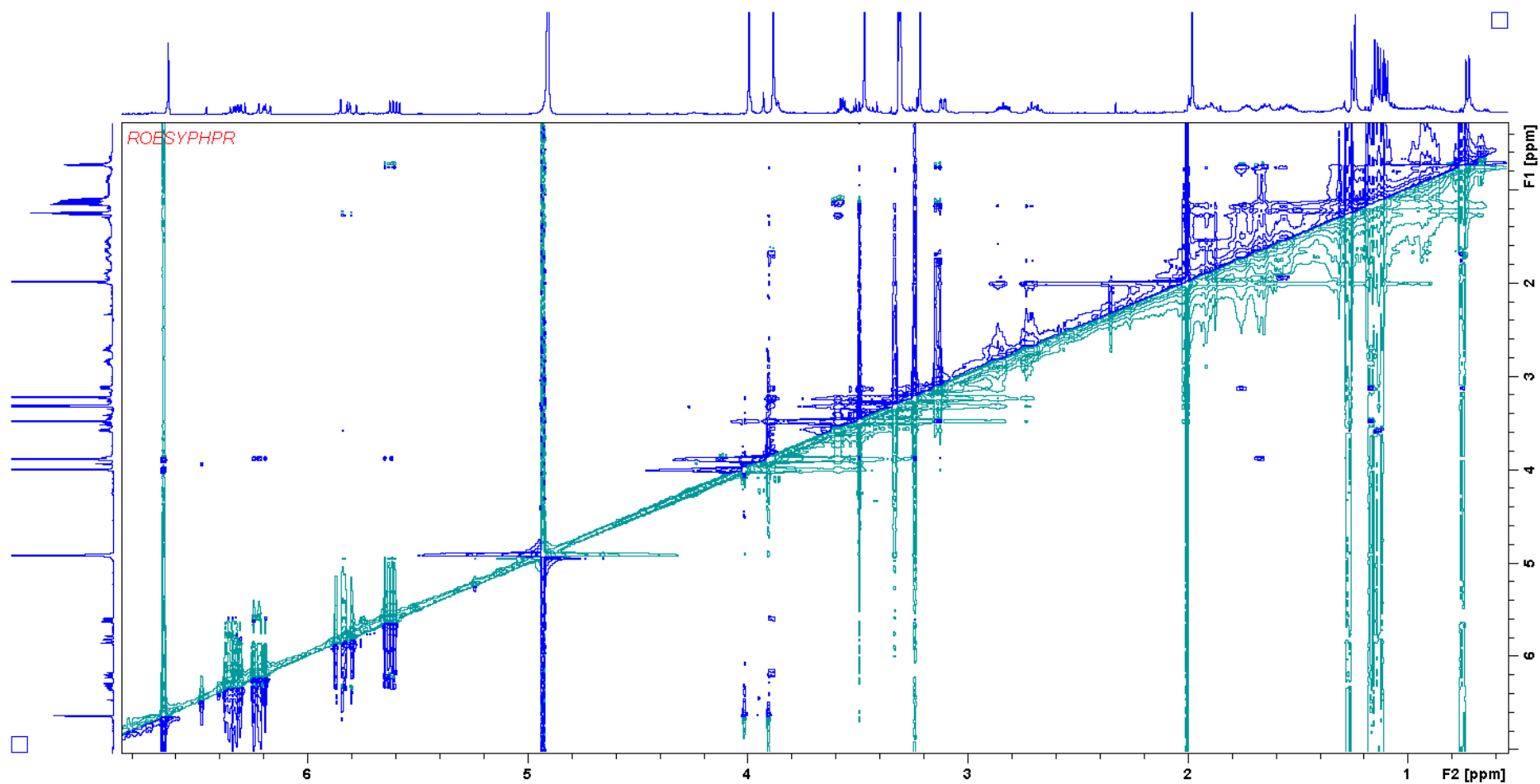


Figure S37. ROESY *phpr* spectrum of stigmatellin C (3) in methanol-d

5. References

1. Gaitatzis, N.; Silakowski, B.; Kunze, B.; Nordsiek, G.; Blöcker, H.; Höfle, G.; Müller, R. The biosynthesis of the aromatic myxobacterial electron transport inhibitor stigmatellin is directed by a novel type of modular polyketide synthase. *J. Biol. Chem.* **2002**, *277*, 13082–13090.
2. Wenzel, S.C.; Müller, R. Myxobacteria - unique microbial secondary metabolite factories. In *Comprehensive Natural Products Chemistry II, Vol 2: Structural Diversity II - Secondary Metabolite Sources, Evolution and Selected Molecular Structures*; Moore, B.S., Ed.; Elsevier: Oxford, 2010; pp 189–222.
3. Keatinge-Clay, A.T. A Tylosin Ketoreductase Reveals How Chirality is Determined in Polyketides. *Chem. Biol.* **2007**, *14*, 898–908.